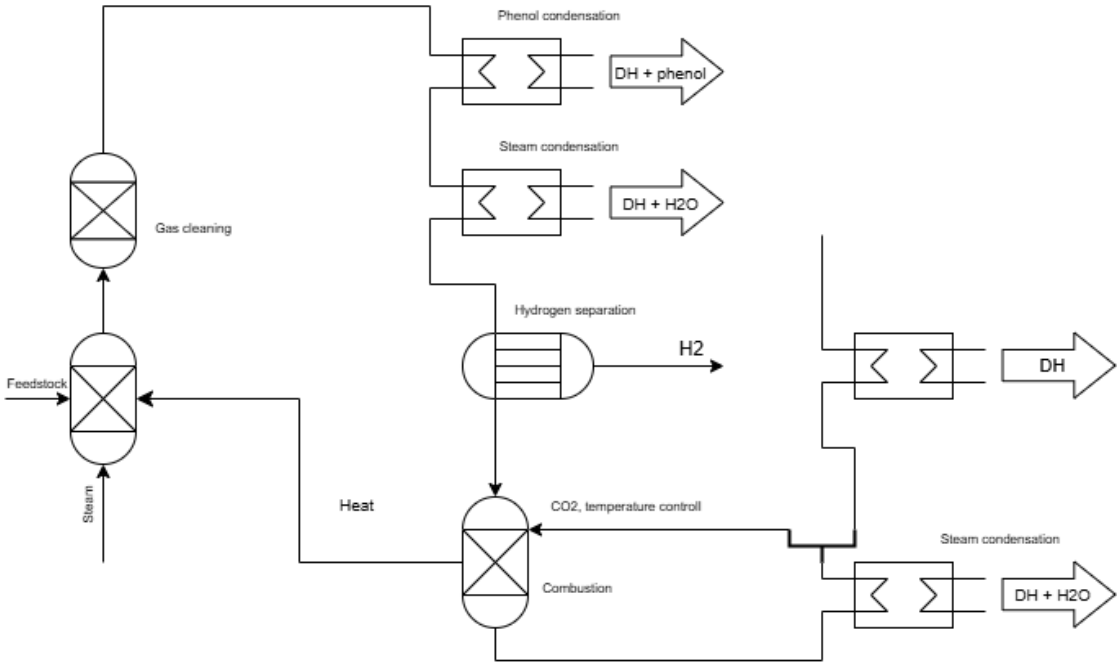

Thermochemical material recovery of wind turbine blades

A techno-economic evaluation of thermochemical conversion as recycling method for end-of-life wind turbine blades

Master's thesis in Sustainable energy systems

Melker Torslén

DEPARTMENT OF SPACE, EARTH AND ENVIRONMENT
CHALMERS UNIVERSITY OF TECHNOLOGY
Gothenburg, Sweden 2025
www.chalmers.se

Master's thesis 2025

Thermochemical material recovery of wind turbine blades

A techno-economic evaluation of thermochemical conversion as recycling method for end-of-life wind turbine blades

Melker Torslén

CHALMERS
UNIVERSITY OF TECHNOLOGY

Department of Space, earth and environment
Division of Energy technology
Chalmers University of Technology
Gothenburg, Sweden 2025

Thermochemical material recovery of wind turbine blades
A techno-economic evaluation of thermochemical conversion as recycling method for end-of-life wind turbine blades
MELKER TORSLÉN

© Melker Torslén, 2025.

Supervisor: Adam Sköld, Department of Space, earth and environment
Examiner: Martin Seemann, Department of Space, earth and environment

Master's Thesis 2025
Department of Space, earth and environment
Division of Energy Technology
Chalmers University of Technology
SE-412 96 Gothenburg
Telephone +46 31 772 1000

Cover: Gasification model flow chart.

Typeset in LaTeX
Printed by Chalmers Reproservice
Gothenburg, Sweden 2026

Thermochemical material recovery of wind turbine blades
A techno-economic evaluation of thermochemical conversion as recycling method for end-of-life wind turbine blades
MELKER TORSLÉN
Department of Space, Earth and Environment
Chalmers University of Technology

Abstract

As the demand for renewable energy increases, more and more wind turbines are constructed as wind power is a proven and cost effective renewable energy source. While most of the turbines are constructed from metal which is fairly simple to recycle, the wind turbine blades are constructed from composite polymer material which is relatively complicated to recycle with products of relatively low value. Currently, the main disposal methods are landfills or incineration. Neither of these options are ideal from an environmental point of view since the polymer material generally is produced from fossil sources. This study is considering an alternative approach, to use thermochemical conversion processes such as gasification and pyrolysis to recover the polymer material. While theoretically possible, this study examines the techno-economical viability of said processes to evaluate if these processes could be commercially feasible as methods to recycle EOL WTB. Using a combination of relatively simple models of distribution of species at equilibrium as well as experimental data the value that can be produced by gasification of feedstock relative to the value that can be produced by incineration can be estimated. Said model indicated that gasification could produce more value than incineration.

Keywords: gasification, EOL WTB, pyrolysis, thermochemical conversion.

Acknowledgements

Firstly I would like to thank Adam Sköld for all the help and support in writing this thesis. Both in terms of the information and insight for gasification you provided and most importantly helping me find a structure and path forwards when information and scope seemed overwhelming and also all the helpful feedback. I would also like to thank Martin Seemann both for taking your time to read and grade this thesis and also for helping me formulate the topic of this thesis. And lastly I would like to thank the gasification group for all the information and feedback you provided.

Melker Torslén, Gothenburg, June 2025

List of Acronyms

Below is the list of acronyms that have been used throughout this thesis listed in alphabetical order:

HHV	Higher Heating Value
SFR	Steam Feedstock Ratio
WTB	Wind Turbine Blade
EOL	End of Life
SMR	Steam Methane Reforming
WGS	Water Gas Shift
PET	Polyethylene Terephthalate
BPA	Bisphenol A
CHP	Combined Heat and Power
HOB	Heat Only Boiler
EUF	Energy Utilization Factor
PUR	Polyurethane
VE	Vinyl Ester
PVC	Polyvinyl Chloride
DH	District Heating

Nomenclature

Below is the nomenclature of indices, sets, parameters, and variables that have been used throughout this thesis.

Indices

p	products
r	reactants
X	unspecified species
H, C	hot- and cold side respectively

Parameters and variables

T	temperature
T_H	hot-side temperature
T_C	cold-side temperature
T_{in}	turbine inlet temperature
$T_{reactor}$	gasification reactor temperature
p	total pressure
p_X	partial pressure of species X
n_X	molar fraction of species X
h_{form}	enthalpy of formation
h_{comb}	enthalpy of combustion
Δh	reaction enthalpy / energy demand
Q_{in}	heat released by combustion of the feedstock
E_{el}	electricity produced
E_{heat}	heat produced
V	value produced by a process
V_{H_2}	value of hydrogen
V_{phenol}	value of phenol
V_{heat}	value of heat
V_{el}	value of electricity
m_{turb}	mass fraction of steam passing through the turbine
η_{HOB}	heat recovery efficiency of the heat-only boiler
η_{el}	electricity generation efficiency
η_{DH}	district heating efficiency
η_{mem}	hydrogen membrane efficiency
f_{el}	fraction of feedstock energy converted to electricity
f_{heat}	fraction of feedstock energy converted to heat
α	power-to-heat ratio
r	ratio of electricity value to heat value
k_p	equilibrium constant based on partial pressures
c_1, c_2	constants in the equilibrium constant correlation

Greek symbols

η	efficiency
η_{HOB}	heat-only boiler efficiency
η_{el}	electricity generation efficiency
η_{DH}	district heating efficiency
η_{mem}	hydrogen membrane efficiency
α	power-to-heat ratio
Δh	reaction enthalpy / energy demand

Contents

List of Acronyms **ix**

Nomenclature **xi**

List of Figures **xvi**

List of Tables **xvii**

1 Introduction **1**
1.1 Aim . . . 2
1.2 Limitations . . . 2
1.3 Specification of the issues being investigated . . . 2

2 Theory **3**
2.1 Material composition of WTB . . . 3
2.2 Thermal decomposition paths . . . 5
2.3 Pyrolysis . . . 6
2.4 Gasification . . . 6
2.5 Reaction energy demand . . . 6
2.6 Economic data for products . . . 6
2.6.1 Economic data for gasification products . . . 6
2.6.2 Economic data for combustion products . . . 7
2.6.3 Hydrogen . . . 8
2.6.4 Phenol . . . 8
2.6.5 District heating . . . 8
2.6.6 Electricity . . . 9
2.7 Hydrogen selective membranes . . . 9

3 Methodology **10**
3.1 Literature study . . . 10
3.1.1 HHV correlations . . . 11
3.1.2 Pyrolysis . . . 11
3.1.3 Gasification . . . 11
3.1.4 Combustion . . . 12
3.2 Reactor modeling . . . 12
3.2.1 Gasification . . . 12
3.2.1.1 Ideal case . . . 13
3.2.1.2 Experimental case . . . 13

3.2.1.3 Equilibrium case . . . 15
3.2.2 Hybrid case . . . 21
3.3 Process modeling . . . 21
3.3.1 Model assumptions . . . 21
3.3.1.1 Comparative cost assumption . . . 21
3.3.1.2 Distribution of species . . . 22
3.3.1.3 Perfect equipment . . . 22
3.3.1.4 Hydrogen handling costs . . . 22
3.3.2 Gasification model . . . 23
3.3.2.1 Model structure . . . 23
3.3.3 Combustion model . . . 26
3.3.3.1 Model structure . . . 26
3.3.3.2 Value of HOB and CHP . . . 27

4 Results **30**
4.1 Comparing value of combustion and gasification . . . 30
4.2 Sensitivity . . . 31
4.2.1 Sensitivity of combustion steam temperature . . . 31
4.2.2 Sensitivity of gasification temperature and SFR . . . 33
4.2.3 Sensitivity of phenol remains . . . 34
4.2.4 H_2 membrane efficiency . . . 34

5 Discussion **36**
5.1 Sensitivity . . . 36
5.2 Factors external to the model . . . 37
5.2.1 Stability . . . 37
5.2.2 Policy and regulation . . . 37
5.3 Future works . . . 37
5.3.1 Model structure . . . 38
5.3.2 Alternative value chains . . . 38
5.3.3 Impact of policy and regulations . . . 38
5.3.4 Material impurities . . . 38
5.3.5 Experimental studies . . . 39

6 Conclusion **40**

Bibliography **41**

A Appendix **I**
A.1 Database_read library . . . I
A.2 HHV_correlations library . . . XII
A.3 gasification_value_range . . . XX

List of Figures

2.1 Material composition distribution of wind turbine blades from different manufacturers by weight 4
2.2 Polyethylene terephthalate molecule 5
2.3 Benzoic acid molecule 5
2.4 Bisphenol-A polymer molecule 5
2.5 Phenol molecule 5

3.1 Equilibrium cases for steam gasification of BPA 18
3.2 Equilibrium cases for steam gasification of PET 19
3.3 Ideal energy demand for gasification equilibrium case 20
3.4 Gasification model structure 23
3.5 Combustion model structure 26
3.6 Combustion value depending on turbine mass fraction T = 450 $°C$ 28
3.7 Combustion value depending on turbine inlet temperature 29

4.1 Relative value of gasification and combustion 30
4.2 Relative value of gasification and combustion dependent on steam temperature 32
4.3 Relative value of gasification and combustion dependent on reactor temperature 33
4.4 Relative value of gasification and combustion dependent on phenol remains in terms of carbon conversion 34
4.5 Relative value of gasification and combustion dependent on membrane efficiency 35

List of Tables

2.1 Ultimate analysis and molar composition of general BPA and PET. 4
2.2 Value ranges used for estimating produced value in the gasification model 7

3.1 Results of ideal cases 13
3.2 Ultimate analysis for experimental feedstock material 14
3.3 Ultimate analysis for experimental feedstock material 14
3.4 Carbon conversion [%] for steam gasification of BPA epoxy at 650 $°C$ . . . 14
3.5 Carbon conversion [%] for steam gasification of BPA epoxy 21
3.6 Base and sensitivity limit values 25

1
Introduction

Wind energy is one of the most used energy sources for electricity production, the third largest source in the EU for 2022, just behind nuclear and gas (The Council of the EU, 2022). It is a vital part of the energy transition, however some problems remain with circularity of materials related to the decommissioning of wind turbines. Most of the materials used in wind turbines, such as steel, aluminum, and exotic materials used in the generator, can be easily recycled and have the economic incentives to do so. The blades consist mainly of composite polymer material that is quite difficult to recycle (Bhatti, 2021). Widely used polymer materials in wind turbine blades are epoxy, polyester, and vinyl ester (Brøndsted et al., 2023). In 2020 the amount of wind turbine blade waste was around 50,000 tons per year, however, in 2050 this number is expected to rise to between 800,000 tons and 2,000,000 tons (Majewski et al., 2022).

There are several methods for the disposal of wind turbine blades; however, one of the most common is still the disposal of the blades in landfills (Bhatti, 2021). Landfill as disposal method has however been banned in EU. As such, the search for disposal methods is becoming increasingly relevant. Ideally, discarded blades should be recycled. Recycling processes can be divided into three categories, mechanical, thermal, and chemical (Khalid et al., 2023).

Within these categories, there are multiple different processes that can be used for recycling. For mechanical recycling, examples of processes are grinding the material to filler materials and cutting the material into segments that could be used in other applications (J. Chen et al., 2019). These processes have the advantages of high technological maturity, low cost, and relative simplicity. However, products from mechanical recycling are limited to products with relatively low value. For thermochemical recycling, the products that can be recovered are of much higher value, such as longer fibers, synthesis gas, and oil (Shen et al., 2023). Examples of thermochemical recycling processes are pyrolysis and gasification. However, these processes have significantly higher energy demand than mechanical recycling processes. Chemical recycling, or solvolysis, also produces products of higher value with potentially higher recovery rate than thermochemical recycling. Solvolysis is, however, a more complicated process that is more sensitive to impurities and often involves environmentally harmful chemicals (Shen et al., 2023), (Khalid et al., 2023).

Given these circumstances, thermochemical recycling could be of interest to explore further. It has the potential to provide a higher value than mechanical recycling

with more circularity of materials. Thermochemical recycling also appears to have less obstacles to expand to the required scale due to solvolysis requiring a feedstock with less impurities.

1.1 Aim

The aim of this study is to gain insight into the economic opportunities and limitations of the value chains of thermochemical recycling processes for wind turbine blades and to determine whether these processes could be economically feasible for commercialization.

1.2 Limitations

- The processes covered in this study will be limited to pyrolysis, gasification and incineration.
- Sweden will be used as a basis for collecting data on energy prices and product values. For cases where data from Sweden can not be obtained data will mainly be obtained from European countries.
- This study will exclusively focus on the relative value produced for pyrolysis, gasification and incineration.
- No experiments will be performed for this study, instead it is limited to literature and modeling.
- The value of the fiber material will not be considered for this study.

1.3 Specification of the issues being investigated

- What are the minimum energy requirements for variations of the investigated processes?
- Are the processes economically viable given current external factors and given reasonable changes of external factors? If not, are there plausible scenarios where the processes would be economically viable?
- If not commercially viable, how costly would the disposal of wind turbine blades be if these processes are required?

2
Theory

2.1 Material composition of WTB

The material used in WTB is mainly a composite of fibers (usually fiberglass) and resin, the polymer is generally mainly composed of polyester or epoxy. Historically polyester were used more prominently due to lower cost, however with turbines getting larger the material choice has shifted towards epoxy due to higher strength (Mishnaevsky Jr et al., 2017). Other fiber materials such as carbon fibers and aramid fibers can also be found in WTB, in smaller amounts, in locations that require higher strength and stiffness. The ratio of resin to fibers in the matrix can range from 0.34 to 0.64 by weight. Which is correspond to 24 wt% resin and 61 wt% fibers for 0.34 as well as 36 wt% resin and 55 wt% fibers for 0.64 (Energy Cluster Denmark, n.d.). In addition to the polymers in the composite matrix, there may be PVC or PUR foam and PUR or VE as adhesives. WTB also usually contains metal with good electrical conductivity such as aluminum or copper for conducting lightning, as well as some steel or aluminum for structural purposes.

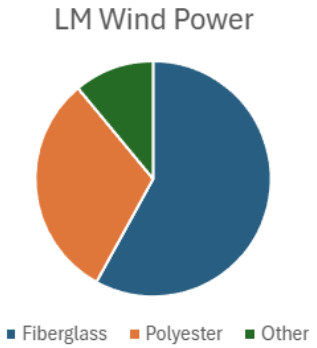

(a) LM wind power

(b) Vestas

(c) Siemens

Figure 2.1: Material composition distribution of wind turbine blades from different manufacturers by weight

The two materials considered are polyethylene terephthalate (PET) and bisphenol-A-based epoxy resin (BPA). These two are chosen due to being the most widely used material in terms of polyesters and epoxy respectively. The composition and heating values for said materials can be found in Table 2.1 (Walters et al., 2000).

Material	C [wt%]	H [wt%]	O [wt%]	HHV $[\frac{MJ}{kg}]$
PET	62.5	4.2	33.3	24.13
BPA	74.09	7.12	18.80	32.28
Material	C $[\frac{mol}{kg}]$	H $[\frac{mol}{kg}]$	O $[\frac{mol}{kg}]$	-
PET	52.04	40.58	20.81	-
BPA	61.69	71.50	11.75	-

Table 2.1: Ultimate analysis and molar composition of general BPA and PET.

2.2 Thermal decomposition paths

Thermal decomposition pathways describe the main chemical transformations that occur when materials, in this case polymers, break down under elevated temperatures. For PET (Figure 2.2) the main product formed is expected to be benzoic acid (Figure 2.3) based on reaction theory and density functional theory (Ma et al., 2022).

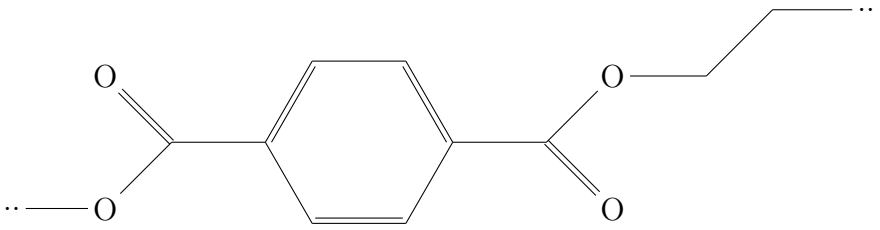

Figure 2.2: Polyethylene terephthalate molecule

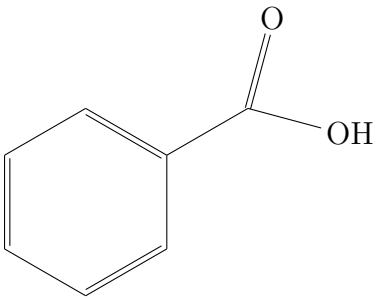

Figure 2.3: Benzoic acid molecule

For BPA (Figure 2.4) the products of the decomposition is mainly BPA monomers and phenol (Figure 2.5) (D'Eusanio et al., 2025). From there the BPA monomers will break down further to mainly phenol, especially in temperatures above 300 $°C$ (Kumagai et al., 2017).

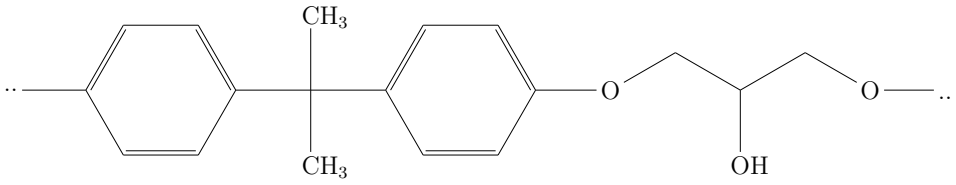

Figure 2.4: Bisphenol-A polymer molecule

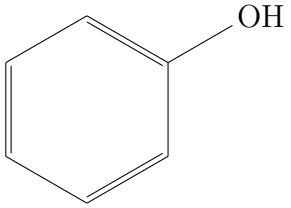

Figure 2.5: Phenol molecule

2.3 Pyrolysis

Pyrolysis is a thermochemical process in which organic matter (or another similar material) decomposes in an environment with elevated temperature and free of oxidizing agents causing large molecules to break down to smaller molecules such as CO, CO_2, CH_4, H_2, C_6H_6 etc. The process usually takes place at 300 $°C$ - 650 $°C$. While pyrolysis produce condensable gases, non-condensable gases and char; the condensable product and char is generally the main product (Basu, 2018).

2.4 Gasification

Gasification refers to the thermochemical conversion process of a solid or liquid carbon based feedstock to gaseous products. In contrast to pyrolysis, gasification often involve a gasification agent such as steam, oxygen, air or CO_2 that reacts with the feedstock. While there often is some amount of liquid products such as tar, the main product is generally gaseous products such as syngas (H_2, CO and CO_2) and some amount of small hydrocarbons (CH_4, C_2H_4 and C_2H_6). Further the temperature of gasification is higher than for pyrolysis, gasification temperatures range from 600 $°C$ - 1200 $°C$ (Y. Zhang et al., 2019). One reaction that have significant impact of the distribution of gaseous products taking place in gasification, especially steam gasification, is the water-gas-shift reaction (WGSR). The WGSR is a redox type equilibrium reaction where CO reacts with H_2O to form CO_2 and H_2. Industrially this reaction has multiple uses including for example syngas production and for removing CO to avoid electrode poisoning in fuel cells (W.-H. Chen and Chen, 2020).

2.5 Reaction energy demand

Using the product distribution, the ideal energy demand for a process can be calculated with the following equation:

$$\Delta h = \sum_p h_{form,p} * n_p - \sum_r h_{form,r} * n_r \tag{2.1}$$

Another case of interest to investigate is extracting only hydrogen and combusting the remaining products to provide energy for the process. For such a case the ideal energy demand can be calculated with the following equation:

$$\Delta h = \sum_p h_{form,p} * n_p - \sum_r h_{form,r} * n_r - \sum_p h_{comb,p} * n_p \tag{2.2}$$

2.6 Economic data for products

2.6.1 Economic data for gasification products

There are three main products to influence value produced, hydrogen gas, phenol and heat. In order for gasification to be a viable market option there are two main

economic constraints. The first constraint is that the gasification process needs to provide equal or greater value per unit mass of feedstock than the values that can be produced with competing processes (in this case heat from combustion). And the second one is that the selling price of hydrogen needs to be equal or lower than the price of competing methods. As such, to properly compare values produced, competitive values of hydrogen are used as a constraint. The same applies to the value of heat.

Table 2.2: Value ranges used for estimating produced value in the gasification model

Product	value range	Unit
H_2	2.5 - 4.8	€/kg
Phenol	0.717	€/kg
District heating	20 - 100	€/MWh

To take into account some margin for error the ranges were expanded slightly wider than the values found.

2.6.2 Economic data for combustion products

There are two common option for generating value with waste incineration. These two options are: heat only boiler (HOB) which only produce district heating and combined heat and power (CHP) also known as cogeneration. Modeling the value produced by the HOB is relatively simple and can be described as the product of heat produced and value of heat with and essentially fixed efficiency.

$$value_{HOB} = value_{heat} * Q_{in} * \eta_{HOB} \tag{2.3}$$

Where Q_{in} is the heat provided by combusting the feedstock, η_{HOB} is the efficiency of the HOB and $value_{heat}$ is the value per unit heat.

Modeling the value produced by CHP is more complicated. The value produced is dependent on the value of heat, the value of electricity, the efficiency of electricity and the efficiency of district heating which both changing depending on the power-heat ratio (α).

$$value_{CHP} = Q_{in} * (value_{el} * \eta_{el} + value_{heat} * \eta_{DH}) \tag{2.4}$$

Which can be rewritten as:

$$value_{CHP} = value_{el} * E_{el} + value_{heat} * E_{heat} \tag{2.5}$$

Where E_{el} and E_{heat} is the electricity and heat produced which can be modeled as

f_{el} and f_{heat}. The model calculates f_{el} and f_{heat} based on the turbine inlet steam temperature as well as the mass fraction of steam in the turbine. Therefore the value of the CHP can be described as:

$$value_{CHP} = value_{el} * f_{el}(T_{in}, m_{turb}) + value_{heat} * f_{heat}(T_{in}, m_{turb}) \tag{2.6}$$

The electricity and heat prices are connected, however the connection is rather complex and depend on a series of market variables. This makes the relation of the prices rather hard to model. To eliminate one unknown variable, scenarios where the prices are set as a ratio to one another will be used.

2.6.3 Hydrogen

Hydrogen is mainly produced with two different methods, these are electrolysis of H_2O and steam methane reforming (SMR). For electrolysis the main cost driver is the cost of electricity, although capital costs are significant, and for SMR the main cost driver is the price of methane with CO_2-costs being somewhat significant (European Comission, n.d.). The European Commission estimates for 2023 the cost of H_2 production for SMR to an European average of 3.76 €/kg with the lowest being in Spain at 2.7 €/kg and 4.8 €/kg for Sweden. For grid-connected electrolysis the average estimated cost is 7.94 €/kg with the lowest being in Finland at 4.1 €/kg with Sweden at 4.4 €/kg. These estimations are based on methane and electricity costs as well as estimated capital costs and efficiencies for the technologies of interest.

Looking at values found in European Hydrogen Valleys, hydrogen "ecosystems" of geographically defined areas, the average value of green hydrogen production is 6.56 €/kg and the average sales price is 6.92 €/kg with the mode value for both being the range 4-6 €/kg (Roland Berger and Inycom, n.d.). The time when these values were acquired were however not specified.

2.6.4 Phenol

The market price in Europe for e-commerce of phenol is 0.717 €/kg (5/5-2025) (ECHEMI Group, n.d.). Since no range of values were found for phenol and it's not a major component considered this will be used as a fixed value. This is not to say that it may not have some significance, however not significant enough to add another range to the calculations due to increased computational time.

2.6.5 District heating

While no data for the operational cost of district heating in Sweden data could be found for Denmark. Which will be used since the costs can be assumed to be similar due to similarities in relevant aspects such as climate, economy and environmental policies. At the lower end, straw-burning boilers were found to have a variable operational cost of 24 €/MWh and at the higher end gas-burning boilers were found to have a variable operational cost of 61 €/MWh of which approximately

half (30.5 €/MWh)were fuel costs (Tian et al., 2019). However, while this study were published in 2019 the source from which the production cost data were taken were accessed in 2017. Since the price of natural gas in Europe increased by ≈ 80 % between 2017 and 2024 it seems likely that the production cost for the gas boilers have increased by at least 24 €/MWh (30.5€/MWh * 0.8 = 24.4€/MWh) to ≈ 85 €/MWh (Eurostat, n.d.).

2.6.6 Electricity

As mentioned earlier to simplify the calculations the value of electricity will be set as a ratio to the heat value, for this three scenarios will be used, r=1, r=2 and r=3 where r is the ratio of electricity value to heat value. The lower boundary, r=1, is used as a lower boundary since producing electricity from heat inevitably will have losses and as such converting heat to electricity is a value loss whenever heat have equal or higher value than electricity. In practice this is more complicated with supply and demand as well as ramp up times etc, however that is beyond the scope of this study. The upper boundary is set since heat pumps (which usually have a COP=3) can produce 3 units of heat per unit electricity (Ariston group, n.d.). The case of r=2 is used as a middle ground.

2.7 Hydrogen selective membranes

Hydrogen selective membranes are, as the name suggests, membranes that let mainly hydrogen gas pass through while preventing flow of other gases. There are several types of membranes based on the material they consist of. These types include polymeric, metallic, carbon, ceramic and mixed-matrix membranes as well as a few more. These different types have different properties and advantages, for example polymeric membranes are typically cheaper while being more permeable but less selective than most other types. Metallic membranes on the other hand are known for being very expensive and incredibly selective but also sensitive to sulfur "poisoning" while ceramic membranes typically sits somewhere in between (Karousos et al., 2023). Other properties that differ between the different types of membranes is the operating temperature. For metallic membranes this ranges from about 200 $°C$ to 650 $°C$ and for polymeric membranes it's typically much lower with the upper side of the temperature range being about 200 $°C$ although this will vary significantly for different polymers (Pal et al., 2020). These membranes can also be combined in stages to gain advantages from different types. For example a polymeric-metallic two stage membrane can be used to gain the selectivity of a metallic membrane while keeping costs low by limiting the required size of metallic membrane. Essentially a certain size of membrane can only handle a certain flow rate, by doing an initial separation with a polymeric membrane a smaller metallic membrane still works for a relatively large flow rate. Systems like this can have a hydrogen recovery rate of above 90 % (Zito et al., 2023).

3
Methodology

To determine and compare the value that can be produced by the thermochemical EOL options, mainly combustion, pyrolysis and gasification, the products from each process needs to be estimated and the value of said products needs to be estimated. To estimate the product distribution a model was constructed based on a literature study considering both experimental values from previous study as well as chemical equilibrium theory. The value of the products were estimated based on publicly available data. Using the data for product distribution as well as the data for product value models for determining value from gasification and combustion were constructed. The general idea of the method in this study is to try to outline the relative values produced from incineration and gasification. And given that waste incineration for energy recovery is a commercially established process and a process currently considered for disposal of EOL WTB in Europe, if gasification can match the values produced from combustion, it warrants further studies into gasification as an alternative.

3.1 Literature study

For this study, three end-of-life (EOL) treatment options were considered: gasification, pyrolysis and combustion. The literature study was primarily conducted to identify experimental data that could be used to estimate the product distributions and energy requirements of the investigated processes. In addition, the literature was used to identify relevant reaction pathways, operating conditions and typical process behavior.

Particular emphasis was placed on studies where the feedstock composition and operating conditions were sufficiently well described to allow the reported results to be related to the materials considered in this study. The available information was assessed based on its suitability for constructing mass and energy balances and for providing reference cases against which the modeling results could be evaluated.

The literature data were used in two main ways. First, experimental results were used as reference cases for evaluating the plausibility of the modelled product distributions. Second, where experimental data were insufficient to construct a complete process model, the literature was used to identify appropriate assumptions, reaction pathways and modeling approaches. The amount and type of information available differed between the investigated processes, which ultimately influenced how each

process could be represented in the modeling.

3.1.1 HHV correlations

In the process of this literature study there were several cases of exact materials being unknown, instead only the elemental mass fractions were known. Since knowing the heat of combustion for several materials were important in this analysis a method of determining this was needed. For unknown materials with a known ultimate analysis the heating value can be estimated with correlations between the atomic composition and the heating value(Channiwala and Parikh, 2002). Some known correlations from the cited study were tested for several polymers with known HHV by calculating HHV based on the correlation and comparing with the known value. The three most accurate where chosen and used in calculations. The correlations chosen were nr 6, 12 and 20 in Table 1 of the cited study.

3.1.2 Pyrolysis

To investigate the products produced from pyrolysis as well as the energy demand, experimental studies were reviewed. It, however, proved difficult to find studies that presented both the material used as feedstock as well as a comprehensive coverage of the products. Most of the studies appeared to focus primarily on the liquid products or specific molecules produced while not comprehensively covering the rest of the products. In practice this meant that a lot of products were not presented at all and the ones that were presented often were grouped such that the distribution could not be determined. An example of this is that in (Torres et al., 2000) $C_1 - C_4$ gases where reported as a group with no indication as to the distribution of each carbon chain length or distribution between alkanes, alkenes and alkynes. In other studies with a more comprehensive coverage of the products such as (Cunliffe and Williams, 2003) the data on the feedstock material were not described in detail. For this reason the heat balance could not be determined. Further the reaction taking place in pyrolysis is rather complicated and difficult to model.

3.1.3 Gasification

Experimental studies on the gasification of epoxy-based materials were reviewed to establish a basis for modeling the gasification of wind turbine blade material. One of the studies considered was (S. Zhang et al., 2012), which investigated the steam gasification of epoxy resin. This study was relevant to this study since steam was considered as the gasifying agent and the study provided experimental data on the resulting gas products.

The literature data were used both to identify the main products that should be considered in the model and to provide a reference case for evaluating the modeled product distribution. The main gaseous products considered in the gasification model were H_2, CO, CO_2, CH_4 and H_2O. However, the experimental data available from the literature were not sufficient to establish a complete mass and energy balance for the process. In particular, not all information required to fully reproduce

the experimental conditions and product distribution was available.

Consequently, the literature data were not used directly as a complete process model. Instead, they were used to establish a suitable basis for the modeling approach. Chemical equilibrium calculations were employed to estimate the distribution of the main gaseous products based on the feedstock composition and process conditions. The experimental results from (S. Zhang et al., 2012) were subsequently used as a reference for assessing whether the predicted product distribution was reasonable.

The comparison between the experimental results and the equilibrium calculations also indicated that equilibrium modeling alone did not capture all experimentally observed products. In particular, phenol was observed in significant quantities in the experimental results but was not represented by the equilibrium model. This motivated the use of a hybrid modeling approach, where the equilibrium model was used to estimate the main gaseous products while experimentally observed condensable products were implemented separately.

3.1.4 Combustion

The combustion process is significantly simpler from a chemical perspective in that there are fewer products and the combustion often is relatively close to an "ideal case" which represents complete combustion where the feedstock is fully oxidated. The products are close to entirely composed of CO_2 and H_2O with small amounts of CO with around 100 mg CO per MJ which for BPA is approximately 3000 mg per kg or around 0.4 % carbon conversion (Naturvårdsverket, 2005). This means that the ideal case is a close approximation for combustion.

3.2 Reactor modeling

Since this study is reliant on knowing the product composition distribution this has to be estimated. Knowing the product composition is required for determining the energy balance of the reactor which is a strong influence on the operational cost. In addition, knowing the product composition is required to the determine the product value which also is vital for the operational economy. A few different approaches are explored as options for modeling the reactor.

3.2.1 Gasification

As mentioned under section 3.1.3 the data found from experimental studies were incomplete and not sufficient to estimate the energy balance. Since the experimental data found were insufficient and performing experiments were outside the scope of this study the reactions needs to be modeled.

3.2.1.1 Ideal case

The first and simplest model tested were ideal cases which refers to the materials converting entirely to certain products. While not the most accurate model its simplicity makes it a useful tool for an initial analysis. The cases explored here are: steam gasification assuming that all carbon is converted to CO, partial oxidation gasification assuming that all carbon is converted to CO and steam gasification assuming that all carbon is converted to CO_2. The cases in which carbon is assumed to be converted to CO represent cases focused on syngas production and the case in which the focus is on maximizing hydrogen production.
While the ideal cases are not strictly realistic the reaction can be controlled to a certain degree via the reactor temperature as well as the partial pressure of steam to shift the chemical equilibrium which can be seen in figure 3.1 and 3.2. This is outlined in Section 3.2.1.3.

Considering these three gasification cases for BPA and using the value data from section 2.6.1 gives the results that can be seen in in Table 3.1. The max value uses the highest value found for H_2 and the highest value for heat 4.8 €/kg and 85 €/MWh respectively. And the same for the min value with 2.5 €/kg and 24 €/MWh respectively.

Table 3.1: Results of ideal cases

	Steam to CO	O_2 to CO	Steam to CO_2	Combustion
H_2 [kg]	0.17	0.07	0.30	0.00
Heat demand [kWh]	2.65	-1.31	2.69	-8.97
CO comb. heat [kWh]	4.88	4.88	-	-
Min value [€]	0.49	0.33	0.67	0.22
Max value [€]	1.02	0.87	1.20	0.76

This gives an indication that there is theoretically a potential for gasification to produce a higher value than combustion. But more importantly, this indicates that focusing on producing H_2 and converting the carbon into CO_2 appears to generate the most value and as such that path is likely most interesting to investigate. To investigate this a more accurate model should be used.

3.2.1.2 Experimental case

While the experimental data on it's own isn't sufficient for the purposes of this study it can still be used as validation of the models to determine if the models appears to be viable. The study found that best matched the material specifications expected for wind turbine blades (using BPA based epoxy) were used as the baseline (S. Zhang et al., 2012).

Table 3.2: Ultimate analysis for experimental feedstock material

*Estimated based on HHV correlations

C $[\frac{mol}{kg}]$	H $[\frac{mol}{kg}]$	O $[\frac{mol}{kg}]$	HHV* $[\frac{MJ}{kg}]$
61.07	74.46	10.97	33.12

Table 3.3: Ultimate analysis for experimental feedstock material

*Estimated based on HHV correlations

For this experimental study a relatively low temperature of 650 $°C$ were used and the steam-feedstock ratio (SFR) is not specified. There was mentions of testing a range of temperatures 600 - 700 $°C$, this however was only for gas volume and reaction rates and the product distribution were only shown for 650 $°C$. The experimental study also considered a catalytic case and a non-catalytic case however only one temperature case were used. 650 $°C$ as used in this experimental study is in the lower range for gasification and borders to what would be used for pyrolysis rather than gasification, for that reason the non-catalytic case is likely not a very good representation for a gasification case. The catalytic case appears to have a distribution of products that is more similar to what would be expected in gasification. The main components of the product distribution from the experimental data can be seen in Table 3.4. This experimental study focused on the carbon conversion and did not specify hydrogen production although it was mentioned that the molar amount of H_2 gas was approximately twice the molar amount of CO_2.

Table 3.4: Carbon conversion [%] for steam gasification of BPA epoxy at 650 $°C$

*The study mention that the amount of CO_2 likely is higher and some of it is thought to have been absorbed in the catalyst

**Only specification provided is carbon based non-condensable gas, since CO and CO_2 is given this likely refers to $C_2 - C_4$ gases

Material	Non-catalytic	Catalytic
CO_2	5.1	41.9*
CO	7.3	4.9
CH_4	7.7	8.5
$Others$**	3.4	5.5
$Phenol$	42.3	19.2

It is worth noting here that there are significant amounts of phenol present for both the catalytic and non-catalytic case, although significantly more in the non-catalytic case. This is likely from partial decomposition of the BPA molecule since the Phenol molecule structure is present in the BPA molecule structure as can be seen in Figure 2.4 and 2.5.

Based on the fact that the catalytic gasification has significantly less phenol than the non-catalytic case, it will be assumed for the purposes of this study that the phenol present in the products is from partial decomposition of the BPA. Further, if this assumption is correct the amount of phenol would likely decrease with increasing temperatures, however this study only considered one temperature (650 $°C$) and as such this could not be verified. This also means insufficient information to estimate the amount of phenol for variation of conditions.

Since no equivalent study were found for PET feedstock it remains unknown if the same happens for PET. Based on the thermal decomposition pathways of PET found in another study, during pyrolysis it seems likely that benzoic acid may occur (Ma et al., 2022). However this decomposition may look different in gasification conditions.

3.2.1.3 Equilibrium case

To make the ideal cases more accurate, the equilibrium cases for the relevant species can be used to estimate a more realistic product distribution. The code used for equilibrium calculations is the equi_solver() function which can be found in Appendix A.1. However, it's worth noting that the model is only run for temperatures up to 800 $°C$, this is due to the model becoming numerically unstable at higher temperatures. The assumptions made here are:

- No heat losses
- Sufficient resident time to reach equilibrium
- No contaminants in the reaction
- All excess heat from the products are recovered
- Temperature is sufficient to break up reactant molecules
- Products are given only from SMR and WGS reactions

Distribution of species
The two main equilibrium reactions for this case are water-gas-shift (WGS) and steam-methane-reforming (SMR). More reactions taking place, but to maintain reasonable computational time, only SMR and WGS were used for these calculations. Another reaction that might take place is the Boudouard reaction where CO_2 reacts with char to form CO in an endothermic reaction which typically moves forwards at about 700 - 900 $°C$ (Lahijani et al., 2015). There is also hydrogasification where hydrogen reacts with char to form methane (Ali et al., 2017). This is just a few of many other reactions. Reactions like this will also produce some amount of tar, however tar will not be considered a product in this case. The reactor in this model also assumes a tar reformer (recirculating tar and gasifying it with steam) and since the energy demand is calculated from the energy values of incoming reactants and the products in the output this will be accounted for in the energy demands for the reactor.

WGS:

$$CO_2 + H_2 \rightleftharpoons CO + H_2O \tag{3.1}$$

SMR:

$$CO + 3H_2 \rightleftharpoons CH_4 + H_2O \tag{3.2}$$

This gives five species with unknown fractions, i.e. five equations are required to solve the equilibrium. These five equations are conservation of mass for C, H and O:

$$nC = nCO + nCO_2 + nCH_4 \tag{3.3}$$

$$nH = nH_2 * 2 + nH_2O * 2 + nCH_4 * 4 \tag{3.4}$$

$$nO = nCO + nCO_2 * 2 + nH_2O \tag{3.5}$$

As well as equilibrium constant equations for WGS and SMR:

$$k_{p,WGS} = \frac{p_{CO} * p_{H_2O}}{p_{CO_2} * p_{H_2}} \tag{3.6}$$

$$k_{p,SMR} = \frac{p_{CH_4} * p_{H_2O}}{p_{CO} * p_{H_2}^3} \tag{3.7}$$

Where p_X is the partial pressure of species X and:

$$k_p = c_1 * e^{(\frac{T}{c_2})} \tag{3.8}$$

c_1 and c_2 are constants specific for each reaction. The partial pressure is estimated based on the ideal gas law where the volumetric fraction and partial pressure correlate to the molar fraction.

$$p_X = p * n_X \tag{3.9}$$

Where n_X is the molar fraction of species X.

This gives a system of equations that depend on the temperature and the distribution of C, H and O. The distribution of C, H and O were given as a function of the ratio of steam/oxygen to feedstock ratio for a given material.

The results from an experimental study regarding steam gasification of epoxy shows that there could be clear similarities between the equilibrium cases shown in Figure 3.1 and the experimental case (S. Zhang et al., 2012). The uncertainties are in regard to the SFR in the experimental study. The temperature is given at 650 $°C$ which is slightly lower than the lowest temperature modeled in i the equilibrium case. However, looking at low temperature and high SFR in Figure 3.1(a) there appears to be similar distribution as for the catalytic case. The non-catalytic case is significantly different however. It is further mentioned in the report that the hydrogen generated were approximately twice the molar amount compared to CO_2 which again seems to be the case in the model. The main difference in gas distribution is the methane that is significantly higher in the equilibrium case for SFR = 5, at higher values for SFR the carbon conversion to methane decreases. Further, the results from this study also shows significant amounts of phenol in the products as well as some amounts of tar.

Equilibrium case data

The graphs in Figure 3.1 gives indications as on how to set the parameters to optimize H_2 production. Looking at the results for BPA, for a SFR of 1 the H_2 production increases with temperature for the entire investigated temperature range, for SFR 2.5 and SFR 5 H_2 production hits a peak at 1053 K and 1038 K respectively. The temperature range investigated is 973 K - 1123 K. Based on the two other SFR cases it seems plausible that there could also be a peak for the SFR 1 placed outside the investigated temperature range. For the investigated range of SFR the H_2 production increase with increasing SFR for all temperatures. This is expected based on the reactions used in the equilibrium model since both the reactions are have hydrogen on one side and steam on the other. In other words: more steam present shifts the reactions towards more hydrogen. The behavior for the PET results are rather similar.

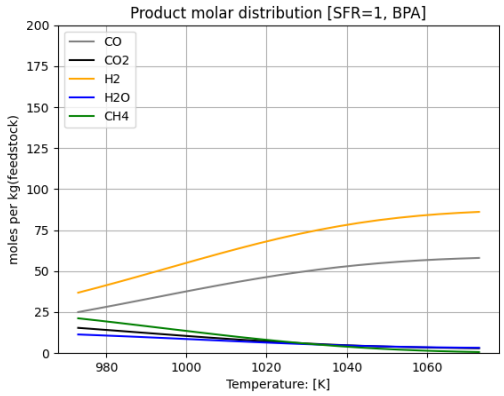

(a) SFR = 1

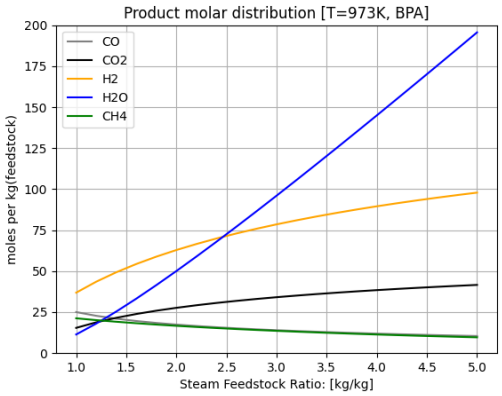

(b) T = 973K

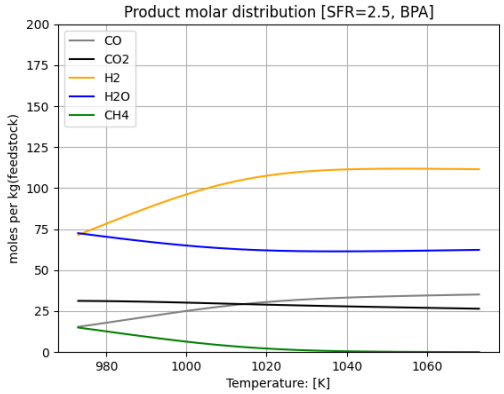

(c) SFR = 2.5

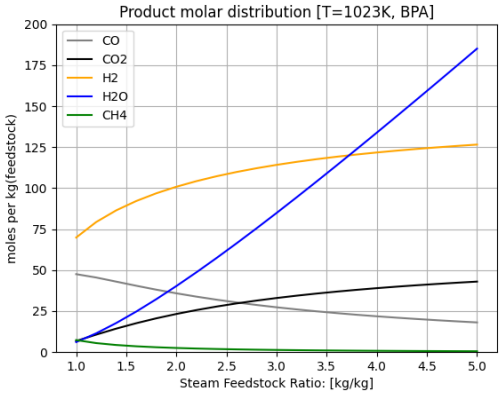

(d) T = 1023K

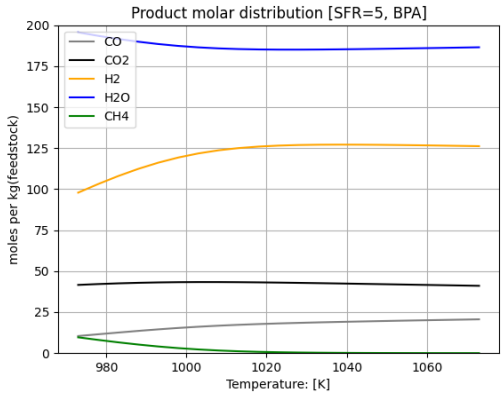

(e) SFR = 5

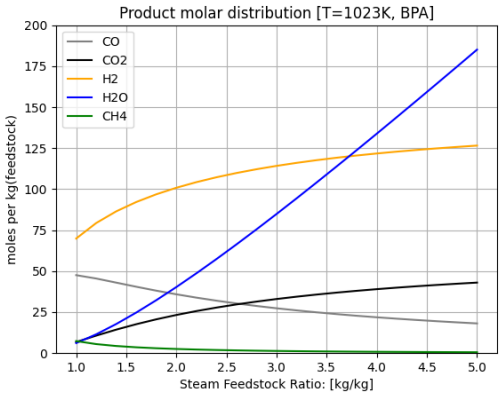

(f) T = 1073K

Figure 3.1: Equilibrium cases for steam gasification of BPA

Similarly for the PET in Figure 3.2 there is a peak temperature for hydrogen production for each SFR. These temperatures are 1063 K, 1033 K and 1023 K for for SFR 1, 2.5 and 5 respectively.

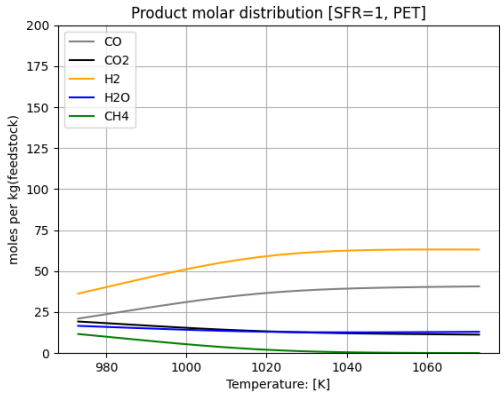

(a) SFR = 1

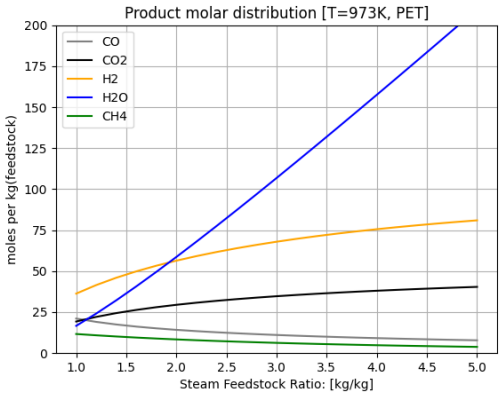

(b) T = 973K

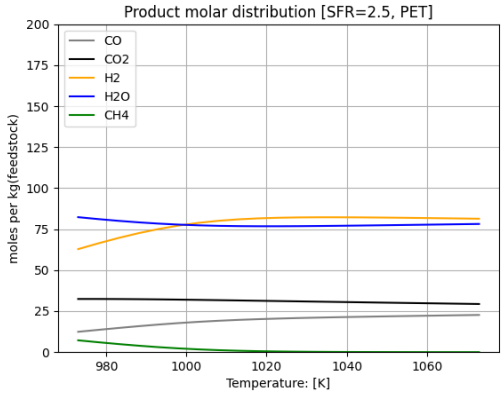

(c) SFR = 2.5

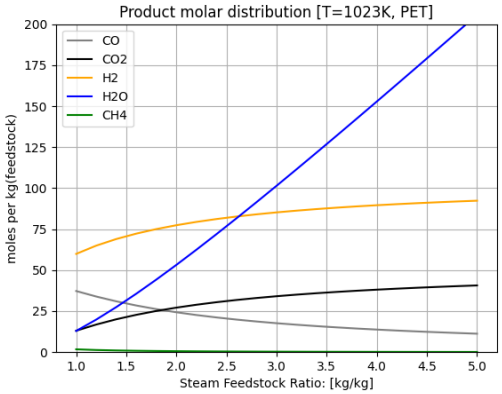

(d) T = 1023K

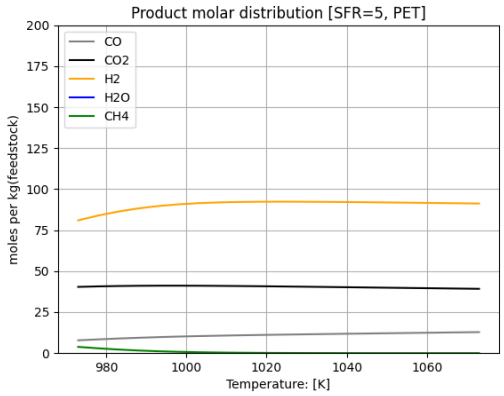

(e) SFR = 5

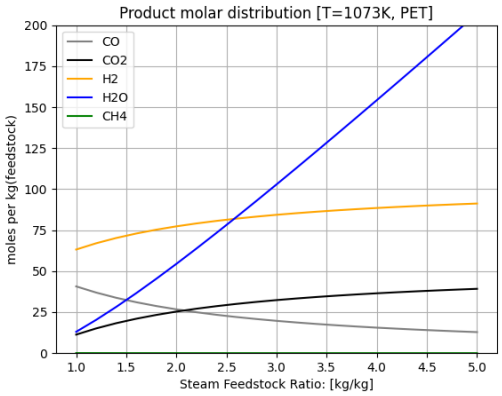

(f) T = 1073K

Figure 3.2: Equilibrium cases for steam gasification of PET

As can be seen in Figure 3.3, the energy demand increases with increasing temperature for all cases. Further the excess gases contain a higher calorific value at lower temperatures resulting in the case of recovering heat through excess gas combustion

appears even better from an energy perspective. However, since it can be seen that the H_2 production is significantly higher at higher temperatures in Figure 3.1 and 3.2, lower temperatures is not necessarily better depending on the relative values.

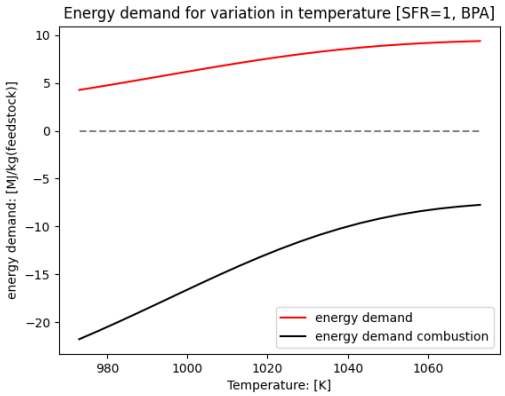

(a) SFR = 1, BPA

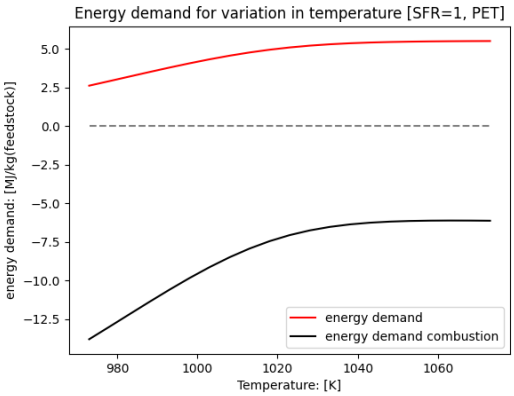

(b) SFR = 1, PET

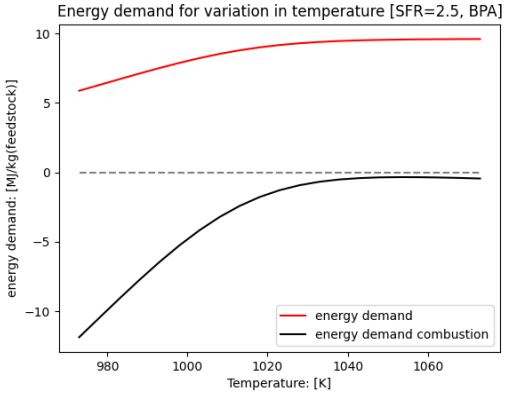

(c) SFR = 2.5, BPA

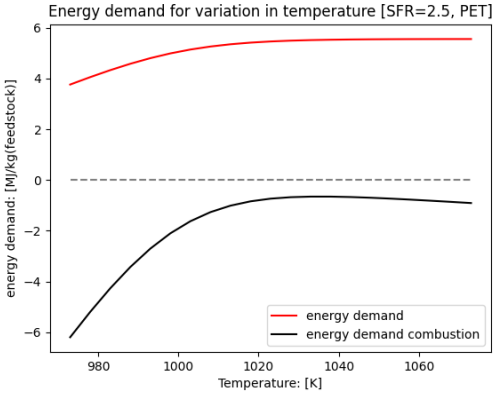

(d) SFR = 2.5, PET

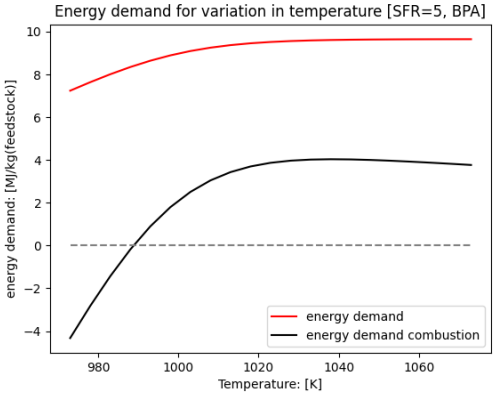

(e) SFR = 5, BPA

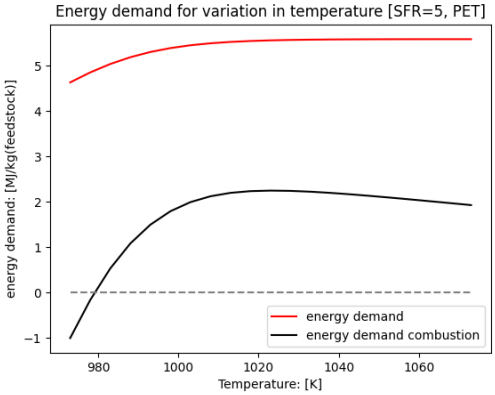

(f) SFR = 5, PET

Figure 3.3: Ideal energy demand for gasification equilibrium case

3.2.2 Hybrid case

Since the experimental data didn't show sufficient information on the distribution of gaseous products and the equilibrium case couldn't estimate the condensable products a hybrid approach was used. The hybrid approach is based on using the equilibrium model to estimate the gaseous products and inserting a fixed value for condensable products such as phenol based on the experimental data.

Table 3.5: Carbon conversion [%] for steam gasification of BPA epoxy

*Equilibrium using T = 650 $°C$ and SFR = 5 and phenol conversion set to 19.2 %

**The study mention that the amount of CO_2 likely is higher and some of it is thought to have been absorbed in the catalyst

***Only specification provided is carbon based non-condensable gas, since CO and CO_2 is given this likely refers to $C_2 - C_4$ gases

Material	Non-catalytic	Catalytic	Hybrid*
CO_2	5.1	41.9**	46.8
CO	7.3	4.9	3.7
CH_4	7.7	8.5	30.4
$Others$***	3.4	5.5	-
$Phenol$	42.3	19.2	19.2

3.3 Process modeling

Based on the hybrid case some models can be constructed to evaluate the economic opportunities of the different methods. As mentioned in the section regarding pyrolysis there is insufficient data to derive a reliable model and as such the two paths that will be examined and compared are gasification and combustion.

3.3.1 Model assumptions

To keep the models at a level of complexity that provide as accurate results as possible while staying within the scope of this work in terms of time certain assumptions and simplifications were made.

3.3.1.1 Comparative cost assumption

Taking the time to model or estimate every cost involved in the investigated processes would be beyond the scope of this work. Instead the economic comparison

between combustion and gasification will be based on the assumption that these processes have an equivalent operational cost. While these costs will not match completely there are similarities that justifies these assumptions. These similarities includes logistics and pre-processing of the feedstock material, similar cleaning of gas both in terms of removal of particulates and corrosive gases as well as handling of solid waste. The upstream supply-chain for the feedstock can be expected to be essentially identical and the equipment required for both processes to be similar, although likely slightly more equipment required for the gasification since more steps are involved mainly in regards to separation of gasification products.

This assumption does come with some limitations, mainly that the values calculated with these models will not be valid for comparison with other processes. Still the values calculated can grant some insight into the potential commercial viability of gasification of EOL WTB. Given that waste incineration for energy recovery is a commercially established process and a process currently considered for disposal of EOL WTB in Europe, if gasification can match the values produced from combustion, it warrants further studies into gasification as an alternative.

3.3.1.2 Distribution of species

The modeling of distribution of species is based on the hybrid approach as specified in section 3.2.2. While this assumption for phenol is likely not very accurate the lack of data for modeling the amounts of phenol in the products necessitates this approach. To compensate for this inaccuracy a large range of amounts of phenol were investigated to determine the impact on the results.

3.3.1.3 Perfect equipment

Assuming equipment heat losses and other losses due to imperfect equipment are small and relatively similar for both processes this can be canceled out for both cases.

3.3.1.4 Hydrogen handling costs

One might also consider compression costs and costs of handling hydrogen gas, however in the case of this study the hydrogen cost is compared against other methods production cost that doesn't account for the handling cost. Therefore including handling costs is not necessary for a comparative cost analysis.

3.3.2 Gasification model

The gasification model was focused around H_2 production for two main reasons.

- There is significantly more data available regarding the value of H_2 and as such the estimated value created from the process will contain less uncertainties.
- By focusing on H_2 production the process of separating the products become significantly simpler by using a membrane for the H_2. The remaining gaseous products have similar boiling points and are of similar sizes complicating their separation processes.

3.3.2.1 Model structure

The process model consists of five main segments, a flowchart for the model can be seen in Figure 3.4. These segments are as follows:

1. Gasification reactor (also includes a tar reformer)
2. Cooling/condensation of liquid products
3. Hydrogen separation (membrane)
4. Combustion of remaining non-condensable gases
5. Cooling/condensation of combustion flue gas

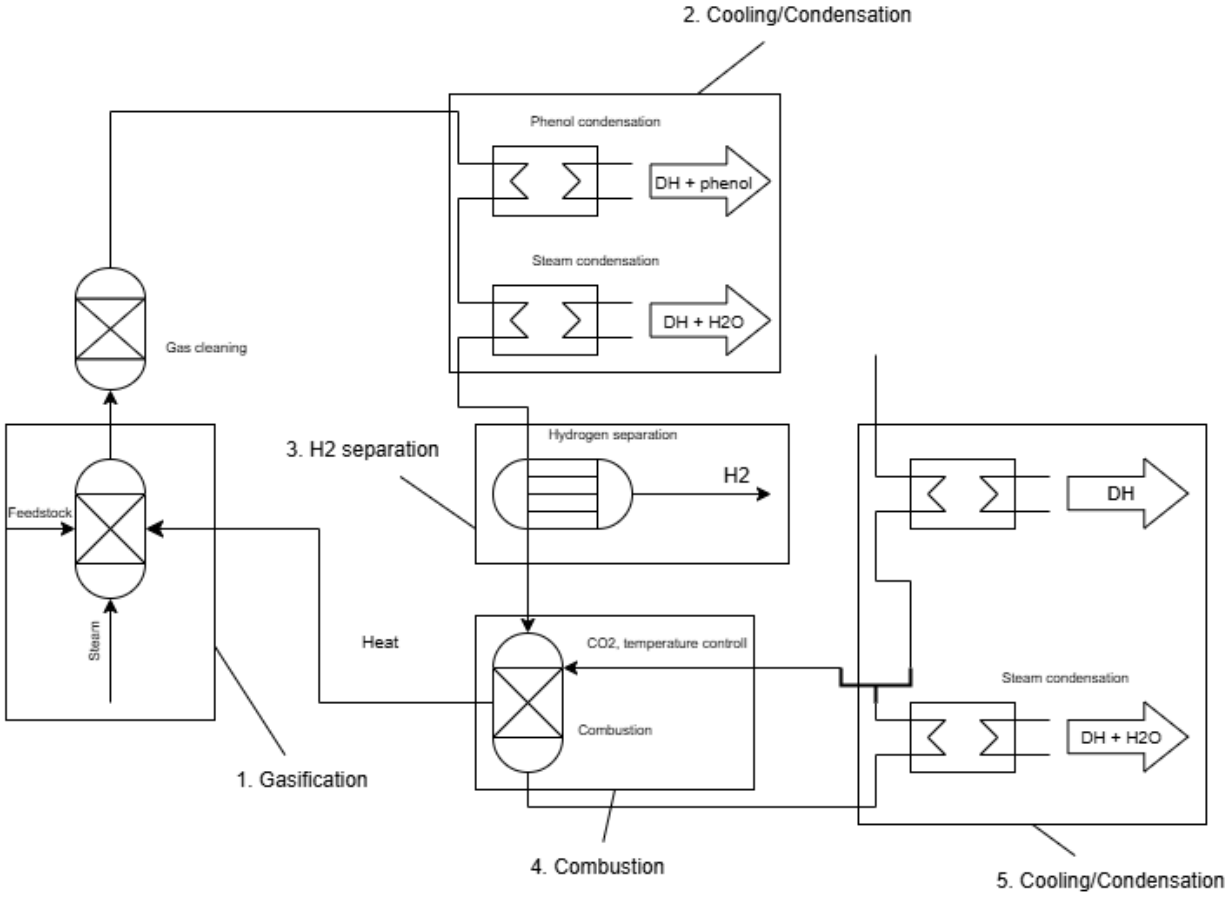

Figure 3.4: Gasification model structure

The code for the model is the gasification_model() function which can be found in Appendix A.1.

1. **Gasification reactor**
   The gasification reactor segment covers the modeling of products resulting from the gasification as well as the energy demand required to drive the reaction, to simplify the model the tar reformer is also included here. The tar reformer refers to a secondary gasification reactor where the tar from the primary reactor reacts with steam to form more syngas. In this model the system boundaries for the gasification reactor was drawn around both reactors. The products are estimated with the hybrid case. Since the estimation for the amount of phenol was not very reliable, performing a sensitivity analysis to determine the impact of different amounts of phenol was the best option available. The energy demand was calculated using the heat of formation for the present species.
2. **Condensation of liquid products**
   The second segment of the model is two steps of heat exchangers, the first one to cool the products to condense the phenol and the second to condense the steam. The excess heat can be used to heat the the feed water for the process. Here the water condensed from the product stream is assumed to not recirculate to the feed water since it likely contains significant amounts of contaminants. Instead, the condensed water is considered to heat exchange with the feed water.
3. **Hydrogen separation**
   In this segment a fraction of the hydrogen is filtered out from the product stream and extracted, the hydrogen extracted here is the the amount considered "produced" from the process. By default the efficiency of the membrane is set to 80%, i.e. 80% of the hydrogen is extracted. This is a realistic number since real systems can achieve a recovery rate of over 90 % as mentioned in Section 2.7. In practice this exact number is dependent on multiple factors such as required purity of the hydrogen, the size of the membrane, temperature and pressure of the feed gas as well as the original hydrogen concentration just to mention a few. Worth noting is that certain materials used for hydrogen membranes have optimal temperatures of operation, depending on what material is chosen further heating or cooling might be required for this step. These optimal temperatures range anywhere from $100\ ^{\circ}C$ to $600\ ^{\circ}C$. However, since the material is not determined in this case and since the energy loss likely is small this is not taken into account in the current model. The reason the energy loss likely is small is that the process doesn't require energy, just a temperature, as a result good insulation and heat exchanging can keep energy losses minimal.
4. **Combustion**
   The combustion segment covers the combustion of the gases remaining after filtering out hydrogen. The remaining combustible gases are mainly CO, CH_4 and H_2. In this model oxy-fuel combustion is used for calculations with recir-

culating CO_2 to manage combustion temperature. Not only does this avoid formation of NOx-gases in the combustion but it also avoids the need to separate the N_2 from the CO_2. There are of course other methods of separating the CO_2 that doesn't involve oxy-fuel combustion, oxy-fuel is however convenient when modeling the product distribution. In practice, considering air combustion with N_2 assumed to be inert is equivalent in terms of the distribution modeling. The combustion temperature is set as $T_{reactor} + 50$ which by default equals 850 $°C$.

5. **Condensation of flue gas**
   The final segment is another case of heat exchanging where the flue gas is cooled to condense the steam. Assuming oxy-fuel combustion the remaining gas should be essentially only CO_2 which can be recirculated to the combustion to control temperature and any excess can be captured and stored or be used for chemical processes such as methanol synthesis.

Base case values
The function making up the gasification model accept seven input parameters. These parameters are reactor temperature, steam fuel ratio, membrane efficiency, phenol remains, value of heat, value of hydrogen and feedstock material. The reactor temperature is set to 800 $°C$, the SFR is set to 1.75 which is the highest value for which the reaction can self sustain with the default values, the membrane efficiency is set to 0.8, the phenol remains is set to 0.336 which represents the phenol remains from the experimental case. The value of heat is set to 80 €/MWh, the value of hydrogen is set to 4.4 and the feedstock material is set to BPA by default.
Product value and sensitivity While the lowest estimated cost of production for hydrogen was 2.7 €/kg one can argue that it might not be the most relevant cost to compare to due to the geographical distance between Spain and Sweden. Looking at countries with the lowest estimated costs with a relatively close geographical proximity to Sweden the costs of 3.2 and 3.4 €/kg for Netherlands and Denmark respectively might be more relevant (Roland Berger and Inycom, n.d.). Other relevant numbers were 4.1 and 4.4 €/kg for electrolytic synthesis of H_2 in Sweden and Finland, these numbers are of interest in a scenario where methane or CO_2 prices increase significantly. Looking at the data from 2022 already shows such a scenario where the lowest estimated costs for SMR were 4.5 €/kg and the lowest cost of grid-connected electrolysis were 3.9 €/kg, which also is a number of interest. This makes the range of interest 3.2 - 4.4 €/kg. This range is supported by the fact that it overlaps with the mode cost range for the Hydrogen Valleys. For this sensitivity analysis the upper and lower limit were given a margin in addition to the highest and lowest value found as shown in Table 3.6.

Table 3.6: Base and sensitivity limit values

Value	Base	Lower	Upper	Unit
H_2	4.4	2.5	4.8	€/kg
Heat	80	20	100	€/MWh

3.3.3 Combustion model

3.3.3.1 Model structure

The combustion model consists of four main segments and is based around a CHP plant but can also model a heat only boiler (HOB) based on the settings. These segments are as follows:

1. Combustion of feedstock
2. Steam turbine with bypass (complete bypass for HOB)
3. Steam condensation
4. Flue gas condensation

The code for the model is the combustion_model() which can be found in Appendix A.1.

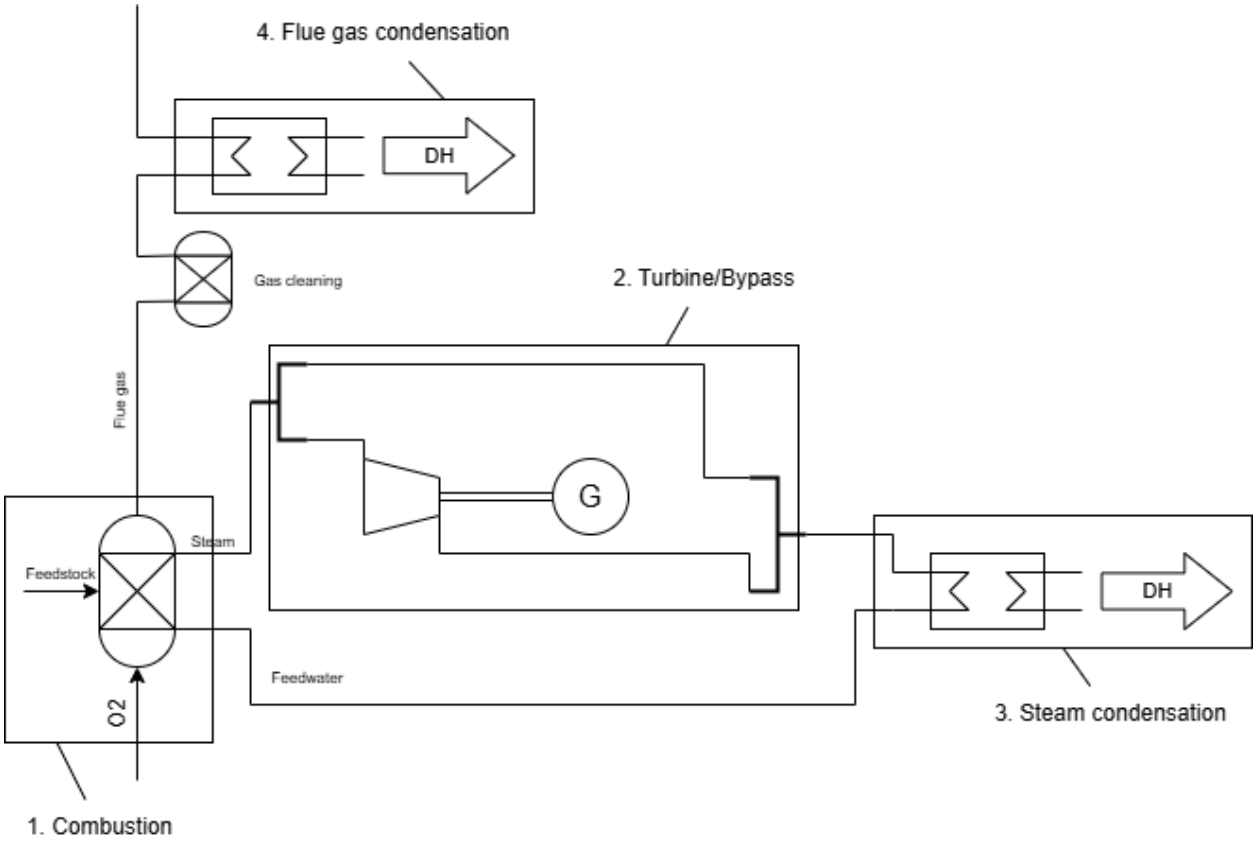

Figure 3.5: Combustion model structure

Combustion
In the combustor for the combustion model similarly as in the gasification model oxy-fuel combustion is used for calculations, assuming the nitrogen remains inert the energy released from combustion is unchanged when using air. The combustion temperature is set as 850 $°C$. The default steam temperature is set to 450 $°C$ which is a common temperature for waste incineration plants (Naturvårdsverket, 2005).

Turbine/Bypass
In this segment production of electricity is calculated, the inlet temperature of the turbine is given by T_{steam} and the outlet temperature is set to 373 K. The efficiency of electricity production is given by the Carnot efficiency as can be seen in equation 3.10. The bypass allows for variation of electricity production by setting the mass fraction of steam passing through the turbine, setting the mass fraction to 0 represents a HOB plant and other cases represents a CHP plant.

$$\eta_{Carnot} = \frac{T_H - T_C}{T_H} \tag{3.10}$$

Steam condensation
This segment models the extraction of heat to district heating. The heat exchanger is assumed to be ideal and the DH temperature is assumed to be 90 $°C$. While an ideal heat exchanger is not realistic this is a loss that will be present in both the gasification and the combustion, since the calculations is purely comparative this does not need to be taken into account.

Flue gas condensation
This par handles the cooling and condensation of flue gas with the same assumptions as for the steam condensation.

Base case values
The function making up the combustion model accept five arguments for variables that can be changed. These arguments are the relative value of electricity and heat, the value of heat, steam temperature at inlet of the turbine, the fraction of steam running through the turbine and feedstock material. The default settings are ratio of electricity and heat value is set to 2, the value heat is set to 80 €/MWh, the steam temperature is set to 450 $°C$, the steam fraction for the turbine is set to 0 (in other words, it is by default a HOB) and the feedstock material is set to BPA which is the more common material.

3.3.3.2 Value of HOB and CHP

Running the combustion model using a range of turbine mass fractions with the above mentioned cases for relative value of electricity and heat gives the following result.

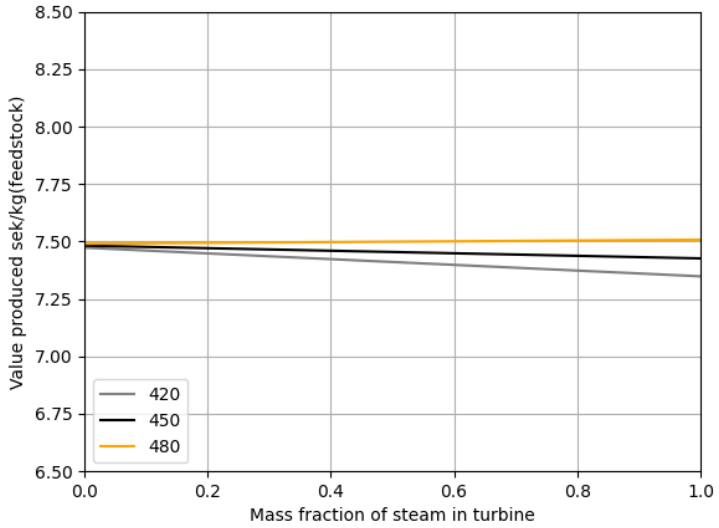

Figure 3.6: Combustion value depending on turbine mass fraction T = 450 $°C$

Based on the graph in Figure 3.6 it can be seen that the value provided from combustion have a linear relationship to the mass fraction of steam flowing through the turbine and the slope depends on the relative value of the electricity and heat. The linearity shows that the maximum value of combustion is always given at one of the borders, or in other words the maximum value provided are constricted to turbine mass fraction = 0 or turbine mass fraction = 1. Further this shows that the maximum value for all $r \leq 2$ are equal for the given settings since for these cases the maximum value is given by the HOB (mass-fraction steam = 0) and as such not influenced by the value of electricity.

However, changing the settings of the combustion model slightly alters this. For example changing the steam temperature alters the slope of the graphs as well as changing the value at turbine mass fraction = 0.

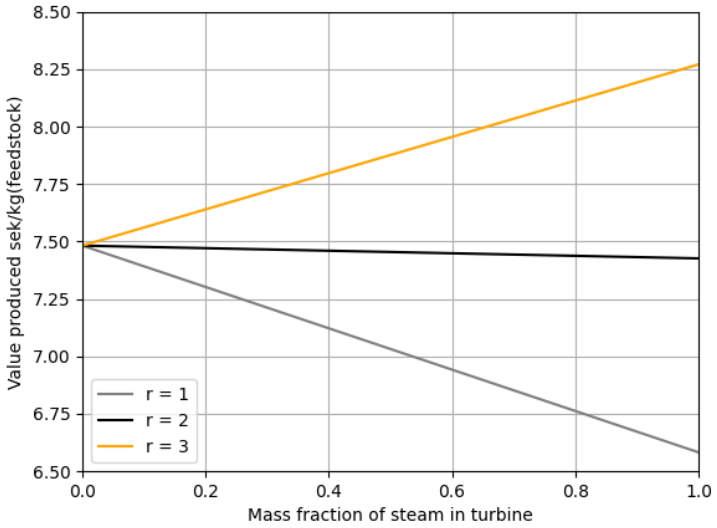

Figure 3.7: Combustion value depending on turbine inlet temperature

It should however be noted that in CHP configuration an incineration plant could provide flexibility and system services which could generate further income, simultaneously CHP plants require significantly more equipment which increase capital costs as well as maintenance cost.

4

Results

4.1 Comparing value of combustion and gasification

To compare the value provided of combustion and gasification the relative results of the models are plotted for a range of values of H_2 and heat using the code found in appendix A.3. Using the default values as well as a range of values for H_2 and heat for sensitivity analysis, the following results are acquired:

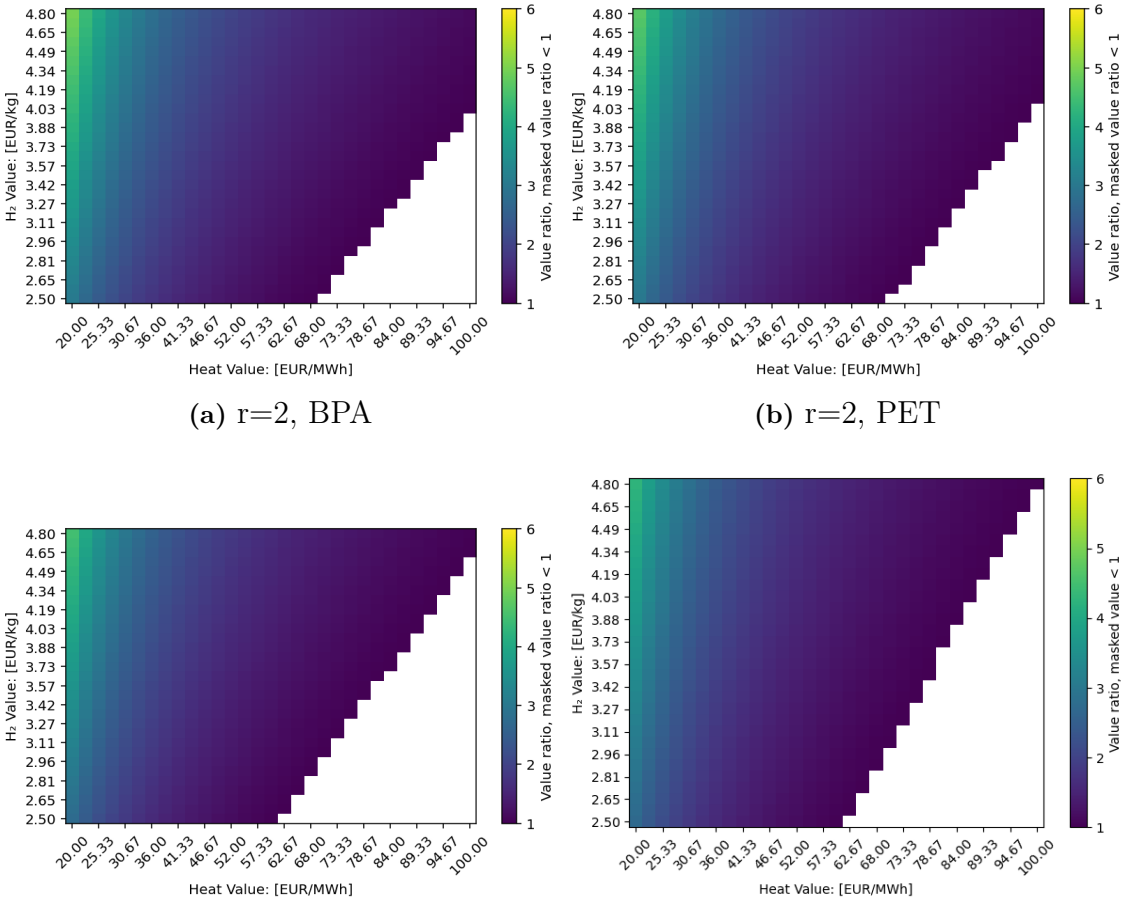

(a) r=2, BPA

(b) r=2, PET

(c) r=3, BPA

(d) r=3, PET

Figure 4.1: Relative value of gasification and combustion

These heat maps show the ratio of the value produced from gasification to the value produced from combustion per kg of feedstock depending on the value of H_2 and DH, the blank areas are cases where the ratio is less than 1 and as such cases where gasification is not economically viable according to the model. In addition to showing for which product values gasification is viable with the given settings these graphs also indicates for which ratio of operational cost between a gasification plant and an incineration plant the gasification could be viable.

4.2 Sensitivity

To evaluate the impact of the uncertainties the model is used for a range of values for the relevant variables to determine if the uncertainties have a notable impact on the results. In this section, for all results the default values are used unless otherwise specified.

4.2.1 Sensitivity of combustion steam temperature

As can be seen in figure 3.7 increasing the steam temperature increases the Carnot efficiency and, as such, increases the value of electricity that can be provided as well as slightly decreasing heat losses. And similarly decreasing steam temperature has the opposite effect. Since the exact temperature is unknown it is of interest to examine how variations impact the result.

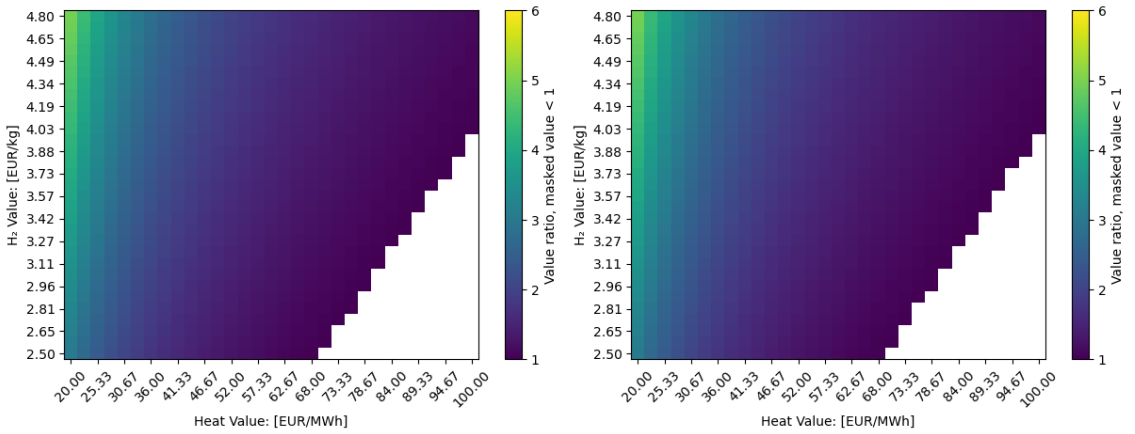

(a) r=1, T=420 °C

(b) r=1, T=480 °C

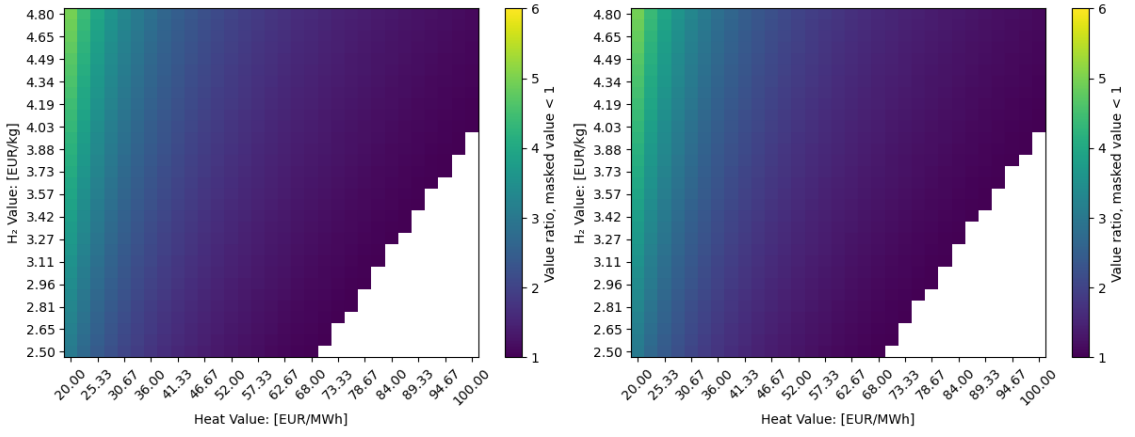

(c) r=2, T=420 °C

(d) r=2, T=480 °C

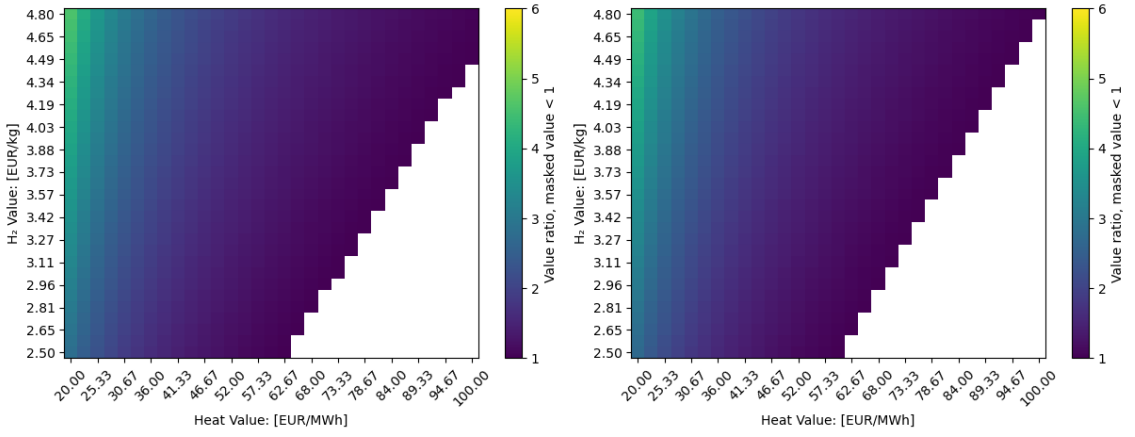

(e) r=3, T=420 °C

(f) r=3, T=480 °C

Figure 4.2: Relative value of gasification and combustion dependent on steam temperature

4.2.2 Sensitivity of gasification temperature and SFR

As can be seen in figure 3.1 and figure 3.3 the energy demand of the reaction as well as hydrogen production increases with increasing reaction temperatures. As such it is of interest to examine the impact of changing the reaction temperatures. For the upper value SFR will be set to the highest possible value while imposing the constraint that the combustion of excess gas provides sufficient heat to meet the energy demand of the reactor and for the lower value SFR will be set to 1. The reason for the upper constraint is to reduce uncertainty. There could conceivably be cases where running the reactor at higher SFR and supply external energy that adds the uncertainty element of one additional unknown operational cost and will therefore not be considered here.

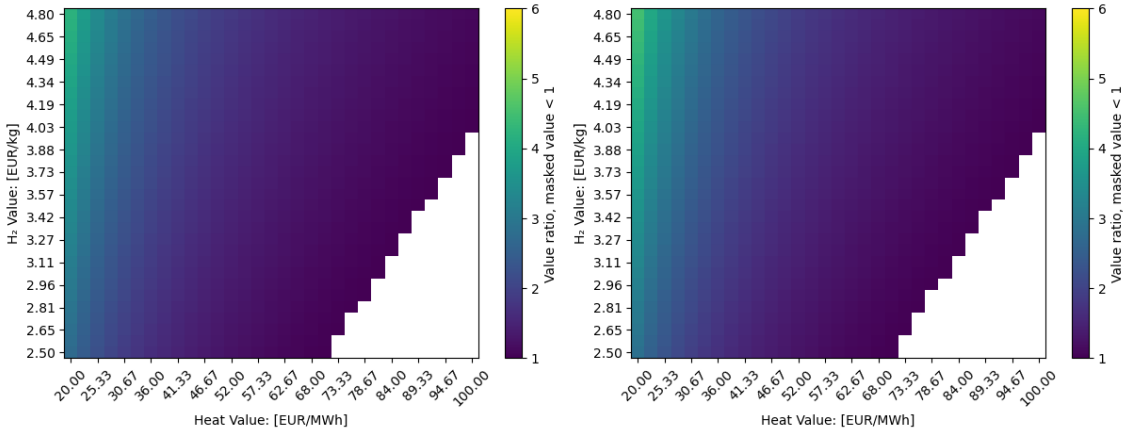

(a) SFR=1, T=750 $°C$

(b) SFR=1, T=850 $°C$

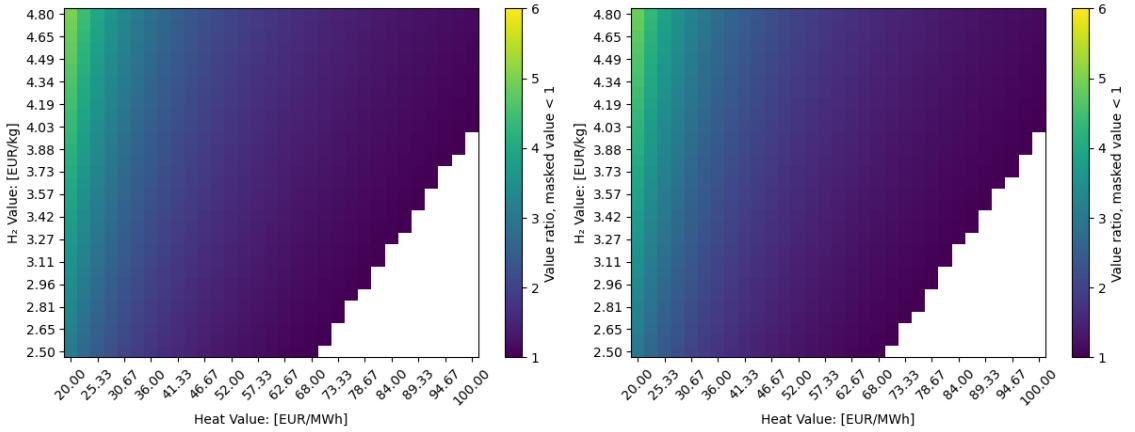

(c) SFR=1.96, T=750 $°C$

(d) SFR=1.66, T=850 $°C$

Figure 4.3: Relative value of gasification and combustion dependent on reactor temperature

4.2.3 Sensitivity of phenol remains

As mentioned earlier, only one study with conditions similar to the gasification process used in this model were found where the phenol remains were given. With only one data point a pattern can't be determined, therefore the entire possible range will be covered in the sensitivity analysis. The upper constraint is based on the assumption that the phenol is formed from parts of the feedstock molecules that isn't completely gasified, with this assumption the upper limit should then theoretically be determined by the fraction of carbon in the feedstock molecule that is bound in the cyclohexane-shapes. The lower limit is simply set to zero. As mentioned in earlier sensitivity analysis, the SFR changes when parameters change due to the imposed constraint that the remaining gases after hydrogen separation should provide sufficient energy when combusted to drive the reaction.

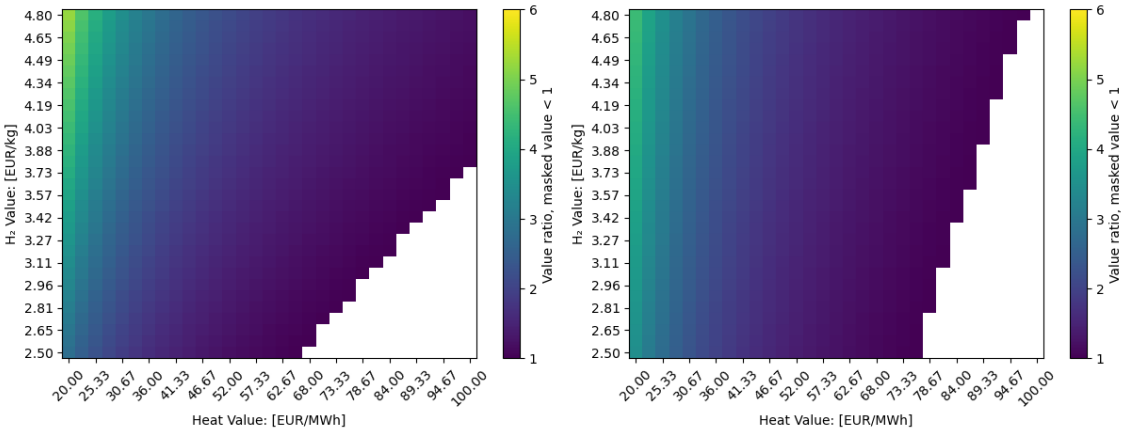

(a) phenol remains=0, SFR = 2.3 **(b)** phenol remains=0.57, SFR = 0.6

Figure 4.4: Relative value of gasification and combustion dependent on phenol remains in terms of carbon conversion

4.2.4 H_2 membrane efficiency

While the membrane efficiency in theory could range anywhere from 0 to 1, with a 0 being a infinitely small membrane and 1 being an infinitely large membrane, in practice this will be trade-off between capital investment cost, operational cost and revenue produced.

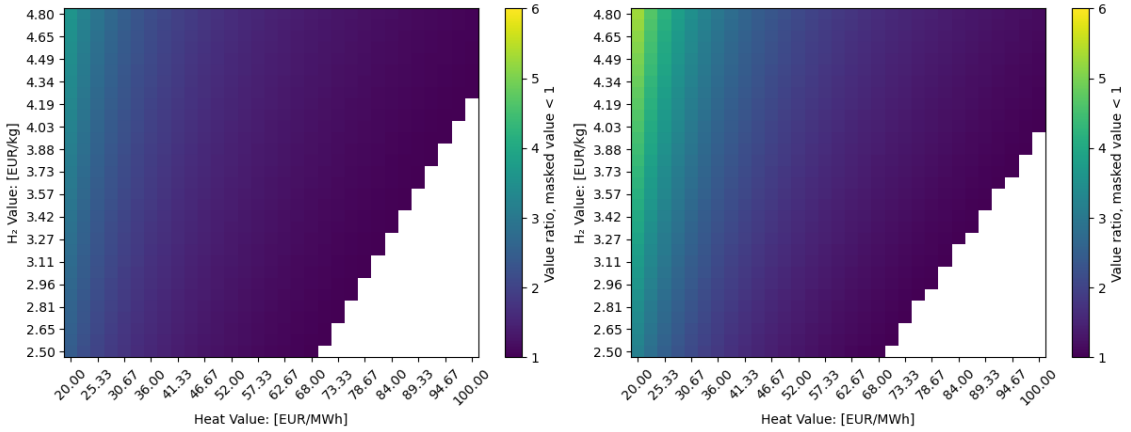

(a) membrane efficiency = 0.4, SFR = 4.9

(b) membrane efficiency = 1.0, SFR = 1.05

Figure 4.5: Relative value of gasification and combustion dependent on membrane efficiency

5
Discussion

5.1 Sensitivity

Increasing the ratio of electricity value and heat value causes a rather noticeable change in the result of the model, which is to be expected given how the model calculates the value produced from combustion. The increase in r results in higher value produced by combustion which decrease the relative value between gasification and combustion. This is the case for both BPA and PET, while PET appears to produce a slightly lower value ratio the difference is likely negligible.

Changing the steam temperature shows no noticeable difference for r = 1 and r = 2, which again remains expected based on figure 3.7 where it can be seen that the maximum value differs less than a percent between the upper and lower temperature, although given the pattern seen in said figure it is likely that further increasing the steam temperature would cause a larger difference. Looking at r = 3 a larger notable difference can be seen with the line where the ratio is equal to one is shifted to the left, which practically means that the required value of H_2 increases and the required value of heat decreases for gasification to be viable.

The temperature of the gasification reactor appears to barely have any impact on the value produced, the SFR on the other hand appears to have slightly more impact. The line where the value ratio is equal to one has a very small shift to the left for lower SFR, the highest values changes more notably and decreases at lower SFR.

The amount of phenol produced does appear to have significant impact on the result, the amount of phenol changed not only the position of the line where the value ratio is equal to one but also the slope of the line. The changing slope in practice means that the sensitivity to value of H_2 and heat changes. Which is expected based on how the model calculates values, since remaining phenol is essentially unreacted material more phenol means less reacted material which means less hydrogen. This means that the value produced is less influenced by the value of hydrogen and more influenced by the value of heat and the value of phenol. While the amount of phenol appears to have more impact than other sensitivity analyses it is worth noting that a significantly wider range is examined for phenol remains due to large uncertainty regarding the likely amount remaining phenol.

The efficiency of the membrane appears to have rather small difference on the position of the line where gasification and combustion produce equal value, however the slope of the line changes slightly. Further the highest ratio of value within the sensitivity range produced increases significantly for a higher efficiency. Depending on the capital cost of the membrane in relation to the capital cost of of the entire plant both a smaller and a larger membrane may be of interest.

5.2 Factors external to the model

The model used in this study covers a limited perspective and as such there are several external factors that are not accounted for in the model which could impact both the comparison between gasification and incineration and between gasification and other methods of hydrogen production.

5.2.1 Stability

A potential advantage of gasification as a method of producing hydrogen is that it could theoretically produce H_2 to relatively stable cost since the method is not heavily dependent on external energy. In case of electrolysis and SMR the cost of production is driven by energy costs to a large extent which may cause significant cost fluctuations. The downside of this is that if electricity prices decrease significantly electrolysis cost may out-compete gasification costs. Further using electrolysis for production of hydrogen can contribute flexible demand for the grid which may generate additional revenue and lowering production cost. Another aspect of stability is the stability of demand combined with possibility of storage. The heat and electricity have limited opportunities of storage and a demand that varies with time of day, day of the week and time of the year. One could argue that hydrogen have better opportunities for storage which gives a more stable demand, that being said, storing hydrogen is not without problems either.

5.2.2 Policy and regulation

There is the possibility that existing or future regulations interfere with thermochemical recycling as a production method depending on how it's interpreted from a legal perspective. For example, it could be interpreted as a method of material recovery which will have one set of regulatory implications. However, it could also be interpreted as hydrogen production with a fossil feedstock which might have a significantly different set of regulatory implications. This may impact the economic value of the products or change requirements for the process. However, this is beyond the scope of this study.

5.3 Future works

This study lays a groundwork to determining if thermochemical recovery of WTBs warrants further studying. There are several other perspectives of this concept that

also should be explored to gain further insight to its viability.

5.3.1 Model structure

As already mentioned, the models used in this study contains multiple simplifications and assumptions that likely decreases the accuracy of the model and the study as a whole, this is to allow for a wider exploration of conditions in the process while maintaining reasonable computational times. The width of the information this study looks at can be used to determine a more narrow range that should be explored with more accurate and computationally intensive models to provide more realistic results.

5.3.2 Alternative value chains

This model focused mainly on hydrogen as source of value due to the reasons mentioned in section 3.3.2, there are however alternatives in terms of value chains. Another option could be to focus on the production of syngas by reacting the CO_2 exit stream with char to form CO which could the be mixed with the H_2 to form syngas, alternatively the CO_2 and H_2 could be reacted to form methanol.

Another value chain of interest to examine further is the fiberglass. While fiberglass is of relatively low value compared to for example carbon fibers it could still provide extra revenue which could be relevant for profitability. Currently this is not taken into consideration with the assumption that incineration and gasification could handle that value stream similarly. It would however be of interest to further study if these two processes have practical differences in the value that could be produced from the fiberglass.

5.3.3 Impact of policy and regulations

As mentioned in Section 5.2.2, the legal interpretation of this process could have significant impact on the economic viability. Therefore, further examination of how this process fits in existing regulatory frameworks (for example EU directives etc) is of significant interest.

5.3.4 Material impurities

In this model impurities are not considered as that complicates the modeling and in practice would likely require experimental studies to determine. In practice the materials will likely have a fairly high degree of impurity, either from long time exposure to environments or from mixed materials being used with additives. For this reason it would be important to further study the effects of impure feedstock material.

5.3.5 Experimental studies

As mentioned in section 3.2.1.2 it turned out difficult to find experimental studies that focused on data relevant for this case. Further experimental studies waste WTB could provide more accurate product estimation and as such more accurate economical comparisons.

6
Conclusion

Based on the findings of this study it appears as if gasification could be a economically viable option for disposal of EOL WTB given the condition that incineration of EOL WTB is economically viable. The value the model suggests could be produced by gasification exceeds the value that the model suggests could be produced by incineration for a wide range of prices for both H_2 and district heating. The sensitivity analyses also shows that these results are robust for changes in multiple key market and operation factors. While this study only covers a rather limited perspective due to the necessary assumptions previously mentioned, the results suggests that further studies on the topic is of interest. Other perspectives of interest to study could be comparative studies regarding operational cost, supply chains integration in a wider recycling system and regulations that may interfere or be beneficial for gasification as a method of EOL WTB disposal.

Bibliography

Ali, D. A., Gadalla, M. A., Abdelaziz, O. Y., Hulteberg, C. P., & Ashour, F. H. (2017). Co-gasification of coal and biomass wastes in an entrained flow gasifier: Modelling, simulation and integration opportunities. *Journal of Natural Gas Science and Engineering*, *37*, 126–137. https://doi.org/https://doi.org/10.1016/j.jngse.2016.11.044

Ariston group. (n.d.). Coefficient of performance of a heat pump: What is it. https://www.ariston.com/en-sa/the-comfort-way/news/coefficient-of-performance-of-a-heat-pump-what-is-it/

Basu, P. (2018). *5 pyrolysis*. https://app.knovel.com/hotlink/khtml/id:kt00CYVHP2/biomass-gasification/biomass-ga-pyrolysis-2

Bhatti, J. (2021). *"europe bans disposal of decommissioned wind turbine blades in landfills: A step towards life cycle sustainability"*. Retrieved January 20, 2025, from https://www.downtoearth.org.in/energy/europe-bans-disposal-of-decommissioned-wind-turbine-blades-in-landfills-a-step-towards-life-cycle-sustainability-77835

Brøndsted, P., Nijssen, R., & Goutianos, S. (2023). *Advances in wind turbine blade design and materials (2nd edition)*. Elsevier.

Channiwala, S., & Parikh, P. (2002). A unified correlation for estimating hhv of solid, liquid and gaseous fuels. *Fuel*, *81*(8), 1051–1063. https://doi.org/https://doi.org/10.1016/S0016-2361(01)00131-4

Chen, J., Wang, J., & Ni, A. (2019). Recycling and reuse of composite materials for wind turbine blades: An overview. *Journal of Reinforced Plastics and Composites*, *38*(12), 567–577. https://doi.org/10.1177/0731684419833470

Chen, W.-H., & Chen, C.-Y. (2020). Water gas shift reaction for hydrogen production and carbon dioxide capture: A review. *Applied Energy*, *258*, 114078. https://doi.org/https://doi.org/10.1016/j.apenergy.2019.114078

Cunliffe, A. M., & Williams, P. T. (2003). Characterisation of products from the recycling of glass fibre reinforced polyester waste by pyrolysis. *Fuel*, *82*(18), 2223–2230. https://doi.org/https://doi.org/10.1016/S0016-2361(03)00129-7

D'Eusanio, V., Rombolà, A. G., Coralli, I., Fabbri, D., Tassi, L., & Marchetti, A. (2025). Thermal degradation pathways in multi-component epoxy composites. *Journal of Analytical and Applied Pyrolysis*, *189*, 107107. https://doi.org/https://doi.org/10.1016/j.jaap.2025.107107

ECHEMI Group. (n.d.). Phenol international price. https://www.echemi.com/pip/phenol-pid_Seven3078.html

Energy Cluster Denmark. (n.d.). Decomblades. https://decomblades.dk/

European Comission. (n.d.). Cost of hydrogen production. https://observatory.clean-hydrogen.europa.eu/hydrogen-landscape/production-trade-and-cost/cost-hydrogen-production

Eurostat. (n.d.). Natural gas price statistics. https://ec.europa.eu/eurostat/statistics-explained/index.php?title=Natural_gas_price_statistics

Karousos, D. S., Qadir, D., Sapalidis, A. A., Ahmad, F., & Favvas, E. P. (2023). Polymeric, metallic and carbon membranes for hydrogen separation: A review. *Gas Science and Engineering*, *120*, 205167. https://doi.org/https://doi.org/10.1016/j.jgsce.2023.205167

Khalid, M. Y., Arif, Z. U., Hossain, M., & Umer, R. (2023). Recycling of wind turbine blades through modern recycling technologies: A road to zero waste. *Renewable Energy Focus*, *44*, 373–389. https://doi.org/https://doi.org/10.1016/j.ref.2023.02.001

Kumagai, S., Ono, S., Yokoyama, S., Kameda, T., & Yoshioka, T. (2017). Fate of bisphenol a pyrolysates at low pyrolytic temperatures. *Journal of Analytical and Applied Pyrolysis*, *125*, 193–200. https://doi.org/https://doi.org/10.1016/j.jaap.2017.04.002

Lahijani, P., Zainal, Z. A., Mohammadi, M., & Mohamed, A. R. (2015). Conversion of the greenhouse gas co2 to the fuel gas co via the boudouard reaction: A review. *Renewable and Sustainable Energy Reviews*, *41*, 615–632. https://doi.org/https://doi.org/10.1016/j.rser.2014.08.034

Ma, T., Wang, R., Wang, W., Gu, W., Yuan, Y., Zhang, A., & Wei, J. (2022). Studies on the thermal degradation mechanism of polyethylene terephthalate and its 2-carboxy ethyl (phenyl) phosphinic acid copolymers. *Polymer Degradation and Stability*, *206*, 110–185. https://doi.org/https://doi.org/10.1016/j.polymdegradstab.2022.110185

Majewski, P., Florin, N., Jit, J., & Stewart, R. A. (2022). End-of-life policy considerations for wind turbine blades. *Renewable and Sustainable Energy Reviews*, *164*. https://doi.org/https://doi.org/10.1016/j.rser.2022.112538

Mishnaevsky Jr, L., Branner, K., Petersen, H., Beauson, J., Mcgugan, M., & Sørensen, B. (2017). Materials for wind turbine blades: An overview. *Materials*, *10*, 1285. https://doi.org/10.3390/ma10111285

Naturvårdsverket. (2005, March). *Förbränningsanläggningar för energiproduktion inklusive rökgaskondensering* (tech. rep. No. 8196) (Utgåva 2). https://www.naturvardsverket.se/globalassets/media/publikationer-pdf/8100/91-620-8196-9.pdf

Pal, N., Agarwal, M., Maheshwari, K., & Solanki, Y. S. (2020). A review on types, fabrication and support material of hydrogen separation membrane [International Conference on Aspects of Materials Science and Engineering]. *Materials Today: Proceedings*, *28*, 1386–1391. https://doi.org/https://doi.org/10.1016/j.matpr.2020.04.806

Roland Berger & Inycom. (n.d.). Hydrogen cost and sales prices. https://h2v.eu/analysis/statistics/financing/hydrogen-cost-and-sales-prices

Shen, Y., Apraku, S. E., & Zhu, Y. (2023). Recycling and recovery of fiber-reinforced polymer composites for end-of-life wind turbine blade management. *Green Chem.*, *25*, 9644–9658. https://doi.org/10.1039/D3GC03479H

The Council of the EU. (2022). *"how is eu electricity produced and sold?"*. Retrieved January 20, 2025, from https://www.consilium.europa.eu/en/infographics/how-is-eu-electricity-produced-and-sold/

Tian, Z., Zhang, S., Deng, J., Fan, J., Huang, J., Kong, W., Perers, B., & Furbo, S. (2019). Large-scale solar district heating plants in danish smart thermal grid: Developments and recent trends. *Energy Conversion and Management*, *189*, 67–80. https://doi.org/https://doi.org/10.1016/j.enconman.2019.03.071

Torres, A., de Marco, I., Caballero, B., Laresgoiti, M., Legarreta, J., Cabrero, M., González, A., Chomón, M., & Gondra, K. (2000). Recycling by pyrolysis of thermoset composites: Characteristics of the liquid and gaseous fuels obtained. *Fuel*, *79*(8), 897–902. https://doi.org/https://doi.org/10.1016/S0016-2361(99)00220-3

Walters, R. N., Hackett, S. M., & Lyon, R. E. (2000). Heats of combustion of high temperature polymers. *Fire and Materials*, *24*(5), 245–252. https://doi.org/https://doi.org/10.1002/1099-1018(200009/10)24:5<245::AID-FAM744>3.0.CO;2-7

Zhang, S., Yoshikawa, K., Nakagome, H., & Kamo, T. (2012). Steam gasification of epoxy circuit board in the presence of carbonates. *Journal of Material Cycles and Waste Management*, *14*. https://doi.org/10.1007/s10163-012-0057-x

Zhang, Y., Cui, Y., Chen, P., Liu, S., Zhou, N., Ding, K., Fan, L., Peng, P., Min, M., Cheng, Y., Wang, Y., Wan, Y., Liu, Y., Li, B., & Ruan, R. (2019). Chapter 14 - gasification technologies and their energy potentials. In M. J. Taherzadeh, K. Bolton, J. Wong, & A. Pandey (Eds.), *Sustainable resource recovery and zero waste approaches* (pp. 193–206). Elsevier. https://doi.org/https://doi.org/10.1016/B978-0-444-64200-4.00014-1

Zito, P. F., Brunetti, A., & Barbieri, G. (2023). Hydrogen concentration and purification by membrane process: A multistage analysis. *Renewable Energy*, *218*, 119243. https://doi.org/https://doi.org/10.1016/j.renene.2023.119243

A

Appendix

A.1 Database_read library

```
import numpy as np
import matplotlib.pyplot as plt
from math import e
from HHV_correlations import *
from sympy.solvers import solve, nsolve
from sympy.abc import a, b, c, d, x


def equi_solver(C, H, O, k1=0.742, k2=0.003909, it=10000):
    if H >= O:
        CO2 = 1
        CH4 = 1
        CO = C - (CO2 + CH4)
        H2O = O - (CO + 2*CO2)
        H2 = (H - (CH4*4 + H2O*2))/2
    if O > H:
        H2O = H*0.5/2
        CH4 = 1
        H2 = (H - CH4*4 - H2O*2)/2
        CO2 = (O - H2O)/(C - CH4) - 1
        CO = C - CO2 - CH4

    for i in range(it):
        if (O - (CO + H2O)) > 0:
            CO2 = (O - (CO + H2O))/2
        else:
            CO2 = 1
            CO -= 1
            H2O -=1

        if (C - (CO2 + CO)) > 0:
            CH4 = C - (CO2 + CO)
        else:
            CH4 = 1
            CO -= 1
```

```
            CO2 -= 1

        if (H - CH4*4 - H2O*2) > 0:
            H2 = (H - CH4*4 - H2O*2)/2
        else:
            H2 = 1
            H2O -= 1
            CH4 -= 1

        if abs((CO*H2O)/(CO2*H2) - k1) > k1*0.0002:
            k =(CO*H2O)/(CO2*H2)
            if k > k1:
                CO -= 0.001
                H2O -= 0.001
            if k < k1:
                CO += 0.001
                H2O += 0.001

        if abs((CH4**(1/3) * H2O**(1/3))/(CO**(1/3) * H2) - k2) >
        ↪  k2*0.0002:
            k = (CH4**(1/3) * H2O**(1/3))/(CO**(1/3) * H2)
            if k > k2:
                CO += 0.001
                H2O -= 0.001
            if (k < k2):
                CO -= 0.001
                H2O += 0.001

    res = nsolve([a+b+x-C, a+2*b+c-O, c+d+2*x-H/2, (a*c)/(b*d)-k1,
    ↪  (x**(1/3) * c**(1/3))/(a**(1/3) * d)-k2], [a, b, c, d, x],
    ↪  [CO, CO2, H2O, H2, CH4], tol=10**-8)

    return(res)



def gen_material_dict(filename):
    materials = {}
    with open(filename, mode='r') as file:
        my_text = file.read()

    text_list = my_text.split('\n\n')
    for text in text_list:
        mat = {}
        rows = text.split('\n')
        if '' in rows:
            rows.remove('')
        for i in range(1, len(rows)):
```

```
            row = rows[i].split(':')
            if row[2] == 'float':
                mat[row[0]] = float(row[1])
            if row[2] == 'int':
                mat[row[0]] = int(row[1])

            materials[rows[0].split(':')[1]] = mat
    return(materials)


def calc_enthalpy(mat:str, data:dict, T=298):
    properties = data[mat]
    dT = T - 298
    H = properties['formation_heat']
    a = properties['a']
    b = properties['b']
    heat = H + a*dT + b*(T**2 - 298**2)
    return(heat)


def calc_from_list(filename:str, mat_dat:dict):
    h_form = 0
    mass = 0
    atomic_balance = {'C':0, 'H':0, 'O':0}
    with open(filename, mode='r') as file:
        my_text = file.read()

    text_list = my_text.split('\n')
    if '' in text_list:
        text_list.remove('')
    for rows in text_list:
        text = rows.split(':')
        mat = mat_dat[text[0]]
        if text[2] == 'mass':
            moles = float(text[1])/(mat['molar_mass']/1000)

        moles = float(text[1])
        h_form += mat['formation_heat']
        atomic_balance['C'] += mat['C']*moles
        atomic_balance['H'] += mat['H']*moles
        atomic_balance['O'] += mat['O']*moles
        mass += moles*mat['molar_mass']/1000

    return(h_form, mass, atomic_balance)


def calc_form_heat_mass(HHV, C, H, O, data):
    C = (C/100)/0.01201
```

```
    H = (H/100)/0.00101
    O = (O/100)/0.016
    n_CO2 = C
    n_H2O = H/2
    n_O2 = (2*C + H/2 - O)/2
    hf_CO2 = data['CO2']['formation_heat']
    hf_H2O = data['H2O']['formation_heat']
    hf_O2 = data['O2']['formation_heat']
    h_form = n_CO2*hf_CO2 + n_H2O*hf_H2O - n_O2*hf_O2 + HHV*1000000
    print('kJ/kg')
    return h_form/1000


def phenol_cp(temp):
    Cp = 24.2 + 0.322*temp - 1.11e-4 * temp**2  # [J/(mol*K)]
    return Cp


def phenol_delta_hvap(temp):
    dH_vap = 102 - 0.184*temp + 1.41e-4 * temp**2   # [kJ/mol]
    return dH_vap*1000      # convert to J/mol and return

def enthalpy_phenol(temp):
    h = 24.2 * (temp - 298) + 0.322 * (temp**2 - 298**2) - 1.11e-4 *
    ↪  (temp**3 - 298**3) - 96400
    return h

def sek_to_eur(sek, eur_sek_ratio=0.091):
    eur = sek*eur_sek_ratio
    return(eur)

def eur_to_sek(eur, eur_sek_ratio=0.091):
    sek = eur/eur_sek_ratio
    return(sek)

def gasification_model(T_r=800, SFR=1.75, n_membrane=0.8,
↪  phenol_remains=0.336, dh_value=80, H2_value=4.4, feed='BPA'):
    f_name = 'material_properties.txt'
    mat_prop = gen_material_dict(f_name)
    # Material data
    h_CO = mat_prop['CO']['formation_heat']
    hc_CO = mat_prop['CO']['combustion_heat']
    h_CO2 = mat_prop['CO2']['formation_heat']
    h_CH4 = mat_prop['CH4']['formation_heat']
    hc_CH4 = mat_prop['CH4']['combustion_heat']
    h_H2 = mat_prop['H2']['formation_heat']
    h_H2O = mat_prop['H2O']['formation_heat']
    T_vap_phenol = 181 + 273    # boiling point for phenol in kelvin
```

```
175     T_vap_H2O = 100 + 273       # boiling point for H2O in kelvin
176
177
178     membrane_efficiency = n_membrane   # fraction of stream hydrogen
        ↪  extracted
179     M_phenol = 6*0.012 + 6*0.00101 + 1*0.016    # molar mass of
        ↪  phenol [kg/mol]
180     total_H2O_out = 0
181     comb_DH_val = 32.2516
182
183
184
185     #
        ↪  ============================================================================
186     # Input section (material input)
187     #
        ↪  ============================================================================
188     if feed == 'BPA':
189         # BPA material
190         C = 61.69
191         H = 70.5
192         O = 11.75
193         h_f = -2106190
194         phenol = 12/21 * phenol_remains * C/6    # mol phenol in
            ↪  producs
195         C -= phenol*6
196         H -= phenol*6
197         O -= phenol*1
198
199     if feed == 'PET':
200         # PET material
201         C = 52.04
202         H = 41.58
203         O = 20.81
204         h_f = -2321330
205         phenol = 6/10 * phenol_remains * C/6    # mol phenol in
            ↪  producs
206         C -= phenol*6
207         H -= phenol*6
208         O -= phenol*1
209
210     T_f = 298       # feedstock input temperature kelvin
211
212
213     # steam feedstock ratio (by mass)
214     nH2O = SFR/0.01802
215     T_steam = 150   # steam input temperature in celcius
216     T_steam += 273  # convert to kelvin
```

```
217     h_steam = calc_enthalpy('H2O_g', mat_prop, T=T_steam)   # steam
        ↪  enthalpy [J/mol]
218     H_steam= h_steam*nH2O
219
220
221     hf_in = h_f + H_steam
222     heating_in = (h_steam - calc_enthalpy('H2O', mat_prop,
        ↪  T=298))*nH2O
223
224
225     #
        ↪  ================================================================================
226     # Gasification reactor section
227     #
        ↪  ================================================================================
228     T_r += 273        # convert to kelvin
229
230
231     c1_wgs = 33.7
232     c2_wgs = -4094
233     kp_wgs = c1_wgs * e**(c2_wgs/T_r)     # Calculate equilibrium
        ↪  constant WGS
234
235
236     c1_smr = 1.63 * 10**(-14)
237     c2_smr = 28116
238     kp_smr = c1_smr * e**(c2_smr/T_r)     # Calculate equilibrium
        ↪  constant SMR
239
240
241     res = equi_solver(C, H + 2*nH2O, O + nH2O, k1=kp_wgs, k2=kp_smr)
242     CO = res[0]
243     CO2 = res[1]
244     CH4 = res[4]
245     H2O = res[2]
246     H2 = res[3]
247
248
249     # output enthalpy
250     H_CO = CO*calc_enthalpy('CO', mat_prop, T=T_r)
251     H_CO2 = CO2*calc_enthalpy('CO2', mat_prop, T=T_r)
252     H_CH4 = CH4*calc_enthalpy('CH4', mat_prop, T=T_r)
253     H_H2 = H2*calc_enthalpy('H2', mat_prop, T=T_r)
254     H_H2O = H2O*calc_enthalpy('H2O_g', mat_prop, T=T_r)
255     H_phenol = enthalpy_phenol(T_r)*phenol
256
257
258     hf_out_r = H_CO + H_CO2 + H_CH4 + H_H2 + H_H2O + H_phenol
```

```
259     reactor_energy_demand = hf_out_r - hf_in
260
261
262     #
        ↪  ==========================================================================
263     # gas cooling
264     #
        ↪  ==========================================================================
265     # phenol condensation
266     T_cool_1 = T_vap_phenol
267
268
269     # output enthalpy
270     H_CO = CO*calc_enthalpy('CO', mat_prop, T=T_cool_1)
271     H_CO2 = CO2*calc_enthalpy('CO2', mat_prop, T=T_cool_1)
272     H_CH4 = CH4*calc_enthalpy('CH4', mat_prop, T=T_cool_1)
273     H_H2 = H2*calc_enthalpy('H2', mat_prop, T=T_cool_1)
274     H_H2O = H2O*calc_enthalpy('H2O_g', mat_prop, T=T_cool_1)
275     # H_phenol = (enthalpy_phenol(T_cool_1) +
        ↪  phenol_delta_hvap(T_cool_1))*phenol
276     H_phenol = (enthalpy_phenol(T_cool_1))*phenol
277
278
279     hf_out_c1 = H_CO + H_CO2 + H_CH4 + H_H2 + H_H2O + H_phenol  #
        ↪  enthalpy of stream before phenol separation
280     cooling_1_energy = hf_out_c1 - hf_out_r
281     hf_out_c1_1 = H_CO + H_CO2 + H_CH4 + H_H2 + H_H2O           #
        ↪  enthalpy of stream after phenol separation
282
283
284     # steam condensation
285     T_cool_2 = T_vap_H2O
286
287
288     # output enthalpy
289     H_CO = CO*calc_enthalpy('CO', mat_prop, T=T_cool_2)
290     H_CO2 = CO2*calc_enthalpy('CO2', mat_prop, T=T_cool_2)
291     H_CH4 = CH4*calc_enthalpy('CH4', mat_prop, T=T_cool_2)
292     H_H2 = H2*calc_enthalpy('H2', mat_prop, T=T_cool_2)
293     H_H2O = H2O*calc_enthalpy('H2O', mat_prop, T=T_cool_2)
294
295
296     hf_out_c2 = H_CO + H_CO2 + H_CH4 + H_H2 + H_H2O     # enthalpy of
        ↪  stream before H2O separation
297     cooling_2_energy = hf_out_c2 - hf_out_c1_1
298     hf_out_c2_1 = H_CO + H_CO2 + H_CH4 + H_H2           # enthalpy of
        ↪  stream after H2O separation
299
```

```
300
301     total_H2O_out += H2O
302
303
304     #
        ↪  ============================================================================
305     # Hydrogen separation and rest-combustion
306     #
        ↪  ============================================================================
307     extracted_H2 = H2*membrane_efficiency
308     H2 = H2*(1 - membrane_efficiency)
309     H_H2 = H2*calc_enthalpy('H2', mat_prop, T=T_cool_2)
310     O2 = CO*0.5 + CH4*2 + H2*0.5
311     H_O2 = calc_enthalpy('O2', mat_prop)
312
313
314     # enthalpy input combustion
315     hf_in_comb = H_CO + H_CO2 + H_CH4 + H_H2 + H_O2
316
317
318     # material output combustion
319     CO2 = CO + CO2 + CH4
320     H2O = CH4*2 + H2
321     H2 = 0
322     CO = 0
323     CH4 = 0
324
325
326     # enthalpy output combustion
327     T_comb = 850 + 273  # combustion temperature in kelvin
328     H_CO2 = CO2*calc_enthalpy('CO2', mat_prop, T=T_comb)
329     H_H2O = H2O*calc_enthalpy('H2O_g', mat_prop, T=T_comb)
330     hf_out_comb = H_H2O + H_CO2
331     energy_output_comb = hf_in_comb - hf_out_comb
332
333
334     # combustion gas cooling
335     T_cool_3 = T_vap_H2O
336     H_CO2 = CO2*calc_enthalpy('CO2', mat_prop, T=T_cool_3)
337     H_H2O = H2O*calc_enthalpy('H2O', mat_prop, T=T_cool_3)
338     hf_cool_3 = H_H2O + H_CO2
339     cooling_3_energy = hf_cool_3 - hf_out_comb
340
341
342     total_H2O_out += H2O
343
344
345     delta_h = []
```

```
346     T_feed = np.linspace(298, 363, 851)
347     for T_water in T_feed:
348         h1 = total_H2O_out*(calc_enthalpy('H2O', mat_prop, T=373) -
            ↪  calc_enthalpy('H2O', mat_prop, T=(T_water+10)))
349         h2 = nH2O*(calc_enthalpy('H2O', mat_prop, T=T_water) -
            ↪  calc_enthalpy('H2O', mat_prop, T=(298)))
350         delta_h.append(abs(h1 - h2))
351
352
353     T_in_w = T_feed[delta_h.index(min(delta_h))]
354     h_H2O = calc_enthalpy('H2O', mat_prop, T=T_in_w)
355
356
357     #
            ↪  ================================================================================
358     # Results
359     #
            ↪  ================================================================================
360     # print('Reactor self-sufficiency factor: ' +
            ↪  str(energy_output_comb/reactor_energy_demand))
361     # print('Steam input heating: ' + str((H_steam - h_H2O*nH2O)/1e6)
            ↪  + ' [MJ/kg(feedstock)]')
362     # print('Gas cooling: ' + str((cooling_1_energy +
            ↪  cooling_2_energy + cooling_3_energy)/1e6) + '
            ↪  [MJ/kg(feedstock)]')
363     DH_val = abs((cooling_1_energy + cooling_2_energy +
            ↪  cooling_3_energy) + (H_steam - h_H2O*nH2O))/1e6 +
            ↪  (energy_output_comb-reactor_energy_demand)/1e6
364     # print('District heating: ' + str(DH_val) + '
            ↪  [MJ/kg(feedstock)]')
365     # print('Produced H2 ' + str(extracted_H2) + '
            ↪  [mol/kg(feedstock)]')
366     # print('Phenol produced: ' + str(phenol*M_phenol) + '
            ↪  [kg/kg(feedstock)]')
367
368
369     #
            ↪  ================================================================================
370     # Produced value
371     #
            ↪  ================================================================================
372     sek_eur_exch = 0.091
373     val_H2 = H2_value/sek_eur_exch              # sek/kg
374     val_phenol = 0.717/sek_eur_exch             # sek/kg
375     val_DH = (dh_value/sek_eur_exch)/3600       # sek/MJ
376
377
```

```
    total_value = (val_H2*extracted_H2*0.00202 + val_phenol*phenol*M_phenol + DH_val*val_DH)
    # print('H2 value produced: ' + str(val_H2*extracted_H2*0.00202) + ' [SEK/kg(Feedstock)]')
    # print('Phenol value produced: ' + str(val_phenol*phenol*M_phenol) + ' [SEK/kg(Feedstock)]')
    # print('DH value produced: ' + str(DH_val*val_DH) + ' [SEK/kg(Feedstock)]')
    # print('Total value produced: ' + str(total_value) + ' [SEK/kg(Feedstock)]')

    return(total_value)


def combustion_model(el_dh_val_ratio=2, value_DH_eur=80, max_steam_temp=450, mass_frac_turb=0, feed='BPA'):
    f_name = 'material_properties.txt'
    mat_prop = gen_material_dict(f_name)


    # Material data
    h_CO = mat_prop['CO']['formation_heat']
    hc_CO = mat_prop['CO']['combustion_heat']
    h_CO2 = mat_prop['CO2']['formation_heat']
    h_CH4 = mat_prop['CH4']['formation_heat']
    hc_CH4 = mat_prop['CH4']['combustion_heat']
    h_H2 = mat_prop['H2']['formation_heat']
    h_H2O = mat_prop['H2O']['formation_heat']
    T_vap_H2O = 100 + 273       # boiling point for H2O in kelvin


    max_steam_temp += 273
    turbine_outlet_temp = 373
    carnot_efficiency = (max_steam_temp - turbine_outlet_temp)/max_steam_temp
    DH_temp = 90 + 273
    feedwater_temp = (DH_temp + 298)/2


    #
    # Input section (material input)
    #
    if feed == 'BPA':
        # BPA material
        C = 61.69
        H = 70.5
```

```
417         O = 11.75
418         h_f = -2106190
419
420     if feed == 'PET':
421         # PET material
422         C = 52.04
423         H = 41.58
424         O = 20.81
425         h_f = -2321330
426
427     h_O2 = calc_enthalpy('O2', mat_prop, T=298)
428     n_O2 = (2*C + H - O)/2
429     H_O2 = n_O2*h_O2
430     hf_in = h_f + H_O2
431
432
433     #
        ↪  ==========================================================================
434     # Combustion
435     #
        ↪  ==========================================================================
436     # Products
437     T_out = 850 + 273
438     n_CO2 = C
439     h_CO2 = calc_enthalpy('CO2', mat_prop, T=T_out)
440     H_CO2 = n_CO2*h_CO2
441     n_H2O = H/2
442     h_H2O = calc_enthalpy('H2O_g', mat_prop, T=T_out)
443     H_H2O = n_H2O*h_H2O
444     hf_prod = (H_H2O + H_CO2)
445
446
447     # Output heat
448     H_out =  hf_in - hf_prod
449     # feedwater flow rate [mol/s]
450     n_feedwater = H_out/(calc_enthalpy('H2O_g', mat_prop,
        ↪  T=max_steam_temp) - calc_enthalpy('H2O', mat_prop,
        ↪  T=feedwater_temp))
451     # Electricity produced J/kg(feedstock)
452     P_el =
        ↪  n_feedwater*carnot_efficiency*mass_frac_turb*(calc_enthalpy('H2O_g',
        ↪  mat_prop, T=max_steam_temp) - calc_enthalpy('H2O_g',
        ↪  mat_prop, T=turbine_outlet_temp))
453     # District heating produced
454     P_heat = n_feedwater*(calc_enthalpy('H2O_g', mat_prop,
        ↪  T=turbine_outlet_temp) - calc_enthalpy('H2O', mat_prop,
        ↪  T=(DH_temp)))
```

```
455     P_heat += n_feedwater*(1 -
        ↪  mass_frac_turb)*(calc_enthalpy('H2O_g', mat_prop,
        ↪  T=max_steam_temp) - calc_enthalpy('H2O_g', mat_prop,
        ↪  T=turbine_outlet_temp))
456     alpha = P_el/P_heat
457     n_el = P_el/H_out
458     EUF = (P_el+P_heat)/H_out
459
460     #
        ↪  ============================================================================
461     # Flue gas cooling
462     #
        ↪  ============================================================================
463     T_out = max_steam_temp + 50
464     h_CO2 = calc_enthalpy('CO2', mat_prop, T=DH_temp)
465     H_CO2 = n_CO2*h_CO2
466     h_H2O = calc_enthalpy('H2O', mat_prop, T=DH_temp)
467     H_H2O = n_H2O*h_H2O
468     P_heat += (hf_prod - (H_H2O + H_CO2))
469
470
471     val_DH = eur_to_sek(value_DH_eur)/3600                    # sek/MJ
472     val_el = val_DH*el_dh_val_ratio                           # sek/MJ
473
474
475     return((P_el/(10**6))*val_el + (P_heat/(10**6))*val_DH)
```

A.2 HHV_correlations library

```
1  def corr_accuracy_molar(HHV, C=0, H=0, O=0, S=0, N=0, A=0, Cl=0):
2      mass = C*12.01 + H*1.01 + O*16.00 + S*32.07 + N*14.01 + A +
       ↪  Cl*35.45
3      C = (C*12.01/mass)*100
4      H = (H*1.01/mass)*100
5      O = (O*16.00/mass)*100
6      S = (S*32.07/mass)*100
7      N = (N*14.01/mass)*100
8      A = A/mass * 100
9      Cl = (Cl*35.45/mass)*100
10
11     corr_dict = {}
12
13     HHV_c = 0.3383*C + 1.443*(H - (O/8)) + 0.0942*S
14     corr_dict['1'] = {'accuracy':(1 - abs(HHV_c-HHV)/HHV),
       ↪  'HHV_c':HHV_c}
15
16     HHV_c = 0.3406*C + 1.443*H - 0.1532*O + 0.1047*S
```

```
    corr_dict['2'] = {'accuracy':(1 - abs(HHV_c-HHV)/HHV),
    ↪  'HHV_c':HHV_c}

    HHV_c = 0.3391*(C - ((3/8)*O)) + 0.2386*(O*3/8) + 1.444*(H -
    ↪  O/16)  + 0.1047*S
    corr_dict['3'] = {'accuracy':(1 - abs(HHV_c-HHV)/HHV),
    ↪  'HHV_c':HHV_c}

    HHV_c = (0.373 - 0.00026*C)*C + 1.444*(H - O/10) + 0.1047*S
    corr_dict['4'] = {'accuracy':(1 - abs(HHV_c-HHV)/HHV),
    ↪  'HHV_c':HHV_c}

    HHV_c = 0.3391*C + 1.4337*H + 0.0931*S - 0.1273*O
    corr_dict['5'] = {'accuracy':(1 - abs(HHV_c-HHV)/HHV),
    ↪  'HHV_c':HHV_c}

    HHV_c = (1.0632 + (1.486e-3)*O)*(C/3 + H - (O - S)/8)
    corr_dict['6'] = {'accuracy':(1 - abs(HHV_c-HHV)/HHV),
    ↪  'HHV_c':HHV_c}

    HHV_c = (0.0152*H + 0.9875)*(C/3 + H - (O - S)/8)
    corr_dict['7'] = {'accuracy':(1 - abs(HHV_c-HHV)/HHV),
    ↪  'HHV_c':HHV_c}

    HHV_c = 0.519*C + 1.625*H + 0.001*O**2 - 17.87
    corr_dict['8'] = {'accuracy':(1 - abs(HHV_c-HHV)/HHV),
    ↪  'HHV_c':HHV_c}

    HHV_c = 0.3403*C + 1.2432*H + 0.0628*N + 0.1909*S - 0.0984*O
    corr_dict['9'] = {'accuracy':(1 - abs(HHV_c-HHV)/HHV),
    ↪  'HHV_c':HHV_c}

    HHV_c = 0.3391*(C - 0.75*(O/2)) + 1.444*(H - 0.125*(O/2)) +
    ↪  0.1047*S
    corr_dict['10'] = {'accuracy':(1 - abs(HHV_c-HHV)/HHV),
    ↪  'HHV_c':HHV_c}

    if O <= 15:
        HHV_c = 0.3361*C + 1.419*H - 0.1453*O + 0.0942*S
    if O > 15:
        HHV_c = 0.3361*C + 1.419*H - (0.1532 - 0.0007*O)*O + 0.0942*S
    corr_dict['11'] = {'accuracy':(1 - abs(HHV_c-HHV)/HHV),
    ↪  'HHV_c':HHV_c}

    HHV_c = 0.3517*C + 1.1626*H + 1.047*S - 0.111*O
    corr_dict['12'] = {'accuracy':(1 - abs(HHV_c-HHV)/HHV),
    ↪  'HHV_c':HHV_c}

```

```
    HHV_c = 0.3414*C + 1.4445*H - (N + O - 1)/8 + 0.093*S
    corr_dict['13'] = {'accuracy':(1 - abs(HHV_c-HHV)/HHV),
    ↪  'HHV_c':HHV_c}

    HHV_c = 0.341*C + 1.323*H + 0.0685 - 0.0153*A - 0.1194*(O + N)
    corr_dict['14'] = {'accuracy':(1 - abs(HHV_c-HHV)/HHV),
    ↪  'HHV_c':HHV_c}

    HHV_c = 0.4373*C - 1.6701
    corr_dict['15'] = {'accuracy':(1 - abs(HHV_c-HHV)/HHV),
    ↪  'HHV_c':HHV_c}

    HHV_c = -0.763 + 0.301*C + 0.525*H + 0.064*O
    corr_dict['16'] = {'accuracy':(1 - abs(HHV_c-HHV)/HHV),
    ↪  'HHV_c':HHV_c}

    HHV_c = 0.328*C + 1.4306*H - 0.0237*N + 0.0929*S - (1 -
    ↪  A/100)*(40.11*H/C) + 0.3466
    corr_dict['17'] = {'accuracy':(1 - abs(HHV_c-HHV)/HHV),
    ↪  'HHV_c':HHV_c}

    HHV_c = 0.352*C + 0.944*H + 0.105*(S - O)
    corr_dict['18'] = {'accuracy':(1 - abs(HHV_c-HHV)/HHV),
    ↪  'HHV_c':HHV_c}

    HHV_c = 0.352*C + 1.507*H - 0.1384*O - 0.1485*C + 0.02419*N +
    ↪  0.09263*S
    corr_dict['19'] = {'accuracy':(1 - abs(HHV_c-HHV)/HHV),
    ↪  'HHV_c':HHV_c}

    HHV_c = 35.8368 + 0.7523*H - 0.2674*S - 0.4654*O - 0.3814*Cl -
    ↪  0.2802*N
    corr_dict['20'] = {'accuracy':(1 - abs(HHV_c-HHV)/HHV),
    ↪  'HHV_c':HHV_c}

    return(corr_dict)


def corr_accuracy_mass(HHV, C=0, H=0, O=0, S=0, N=0, A=0, Cl=0):
    mass = C + H + O + S + N + A + Cl
    C = (C/mass)*100
    H = (H/mass)*100
    O = (O/mass)*100
    S = (S/mass)*100
    N = (N/mass)*100
    A = A/mass * 100
    Cl = (Cl/mass)*100

```

```
    corr_dict = {}

    HHV_c = 0.3383*C + 1.443*(H - (O/8)) + 0.0942*S
    corr_dict['1'] = {'accuracy':(1 - abs(HHV_c-HHV)/HHV),
    ↪  'HHV_c':HHV_c}

    HHV_c = 0.3406*C + 1.443*H - 0.1532*O + 0.1047*S
    corr_dict['2'] = {'accuracy':(1 - abs(HHV_c-HHV)/HHV),
    ↪  'HHV_c':HHV_c}

    HHV_c = 0.3391*(C - ((3/8)*O)) + 0.2386*(O*3/8) + 1.444*(H -
    ↪  O/16)  + 0.1047*S
    corr_dict['3'] = {'accuracy':(1 - abs(HHV_c-HHV)/HHV),
    ↪  'HHV_c':HHV_c}

    HHV_c = (0.373 - 0.00026*C)*C + 1.444*(H - O/10) + 0.1047*S
    corr_dict['4'] = {'accuracy':(1 - abs(HHV_c-HHV)/HHV),
    ↪  'HHV_c':HHV_c}

    HHV_c = 0.3391*C + 1.4337*H + 0.0931*S - 0.1273*O
    corr_dict['5'] = {'accuracy':(1 - abs(HHV_c-HHV)/HHV),
    ↪  'HHV_c':HHV_c}

    HHV_c = (1.0632 + (1.486e-3)*O)*(C/3 + H - (O - S)/8)
    corr_dict['6'] = {'accuracy':(1 - abs(HHV_c-HHV)/HHV),
    ↪  'HHV_c':HHV_c}

    HHV_c = (0.0152*H + 0.9875)*(C/3 + H - (O - S)/8)
    corr_dict['7'] = {'accuracy':(1 - abs(HHV_c-HHV)/HHV),
    ↪  'HHV_c':HHV_c}

    HHV_c = 0.519*C + 1.625*H + 0.001*O**2 - 17.87
    corr_dict['8'] = {'accuracy':(1 - abs(HHV_c-HHV)/HHV),
    ↪  'HHV_c':HHV_c}

    HHV_c = 0.3403*C + 1.2432*H + 0.0628*N + 0.1909*S - 0.0984*O
    corr_dict['9'] = {'accuracy':(1 - abs(HHV_c-HHV)/HHV),
    ↪  'HHV_c':HHV_c}

    HHV_c = 0.3391*(C - 0.75*(O/2)) + 1.444*(H - 0.125*(O/2)) +
    ↪  0.1047*S
    corr_dict['10'] = {'accuracy':(1 - abs(HHV_c-HHV)/HHV),
    ↪  'HHV_c':HHV_c}

    if O <= 15:
        HHV_c = 0.3361*C + 1.419*H - 0.1453*O + 0.0942*S
    if O > 15:
        HHV_c = 0.3361*C + 1.419*H - (0.1532 - 0.0007*O)*O + 0.0942*S
```

```
125     corr_dict['11'] = {'accuracy':(1 - abs(HHV_c-HHV)/HHV),
        ↪  'HHV_c':HHV_c}
126
127     HHV_c = 0.3517*C + 1.1626*H + 1.047*S - 0.111*O
128     corr_dict['12'] = {'accuracy':(1 - abs(HHV_c-HHV)/HHV),
        ↪  'HHV_c':HHV_c}
129
130     HHV_c = 0.3414*C + 1.4445*H - (N + O - 1)/8 + 0.093*S
131     corr_dict['13'] = {'accuracy':(1 - abs(HHV_c-HHV)/HHV),
        ↪  'HHV_c':HHV_c}
132
133     HHV_c = 0.341*C + 1.323*H + 0.0685 - 0.0153*A - 0.1194*(O + N)
134     corr_dict['14'] = {'accuracy':(1 - abs(HHV_c-HHV)/HHV),
        ↪  'HHV_c':HHV_c}
135
136     HHV_c = 0.4373*C - 1.6701
137     corr_dict['15'] = {'accuracy':(1 - abs(HHV_c-HHV)/HHV),
        ↪  'HHV_c':HHV_c}
138
139     HHV_c = -0.763 + 0.301*C + 0.525*H + 0.064*O
140     corr_dict['16'] = {'accuracy':(1 - abs(HHV_c-HHV)/HHV),
        ↪  'HHV_c':HHV_c}
141
142     HHV_c = 0.328*C + 1.4306*H - 0.0237*N + 0.0929*S - (1 -
        ↪  A/100)*(40.11*H/C) + 0.3466
143     corr_dict['17'] = {'accuracy':(1 - abs(HHV_c-HHV)/HHV),
        ↪  'HHV_c':HHV_c}
144
145     HHV_c = 0.352*C + 0.944*H + 0.105*(S - O)
146     corr_dict['18'] = {'accuracy':(1 - abs(HHV_c-HHV)/HHV),
        ↪  'HHV_c':HHV_c}
147
148     HHV_c = 0.352*C + 1.507*H - 0.1384*O - 0.1485*C + 0.02419*N +
        ↪  0.09263*S
149     corr_dict['19'] = {'accuracy':(1 - abs(HHV_c-HHV)/HHV),
        ↪  'HHV_c':HHV_c}
150
151     HHV_c = 35.8368 + 0.7523*H - 0.2674*S - 0.4654*O - 0.3814*Cl -
        ↪  0.2802*N
152     corr_dict['20'] = {'accuracy':(1 - abs(HHV_c-HHV)/HHV),
        ↪  'HHV_c':HHV_c}
153
154     return(corr_dict)
155
156
157 def corr_HHV_mass(C=0, H=0, O=0, S=0, N=0, A=0, Cl=0):
158     mass = C + H + O + S + N + A + Cl
159     C = (C/mass)*100
```

```
    H = (H/mass)*100
    O = (O/mass)*100
    S = (S/mass)*100
    N = (N/mass)*100
    A = A/mass * 100
    Cl = (Cl/mass)*100

    corr_dict = {}

    corr_dict['1'] = 0.3383*C + 1.443*(H - (O/8)) + 0.0942*S

    corr_dict['2'] = 0.3406*C + 1.443*H - 0.1532*O + 0.1047*S

    corr_dict['3'] = 0.3391*(C - ((3/8)*O)) + 0.2386*(O*3/8) +
    ↪  1.444*(H - O/16)  + 0.1047*S

    corr_dict['4'] = (0.373 - 0.00026*C)*C + 1.444*(H - O/10) +
    ↪  0.1047*S

    corr_dict['5'] = 0.3391*C + 1.4337*H + 0.0931*S - 0.1273*O

    corr_dict['6'] = (1.0632 + (1.486e-3)*O)*(C/3 + H - (O - S)/8)

    corr_dict['7'] = (0.0152*H + 0.9875)*(C/3 + H - (O - S)/8)

    corr_dict['8'] = 0.519*C + 1.625*H + 0.001*O**2 - 17.87

    corr_dict['9'] = 0.3403*C + 1.2432*H + 0.0628*N + 0.1909*S -
    ↪  0.0984*O

    corr_dict['10'] = 0.3391*(C - 0.75*(O/2)) + 1.444*(H -
    ↪  0.125*(O/2)) + 0.1047*S

    if O <= 15:
        HHV_c = 0.3361*C + 1.419*H - 0.1453*O + 0.0942*S
    if O > 15:
        HHV_c = 0.3361*C + 1.419*H - (0.1532 - 0.0007*O)*O + 0.0942*S
    corr_dict['11'] = HHV_c

    corr_dict['12'] = 0.3517*C + 1.1626*H + 1.047*S - 0.111*O

    corr_dict['13'] = 0.3414*C + 1.4445*H - (N + O - 1)/8 + 0.093*S

    corr_dict['14'] = 0.341*C + 1.323*H + 0.0685 - 0.0153*A -
    ↪  0.1194*(O + N)

    corr_dict['15'] = 0.4373*C - 1.6701

```

```
203     corr_dict['16'] = -0.763 + 0.301*C + 0.525*H + 0.064*O
204
205     corr_dict['17'] = 0.328*C + 1.4306*H - 0.0237*N + 0.0929*S - (1 -
        ↪  A/100)*(40.11*H/C) + 0.3466
206
207     corr_dict['18'] = 0.352*C + 0.944*H + 0.105*(S - O)
208
209     corr_dict['19'] = 0.352*C + 1.507*H - 0.1384*O - 0.1485*C +
        ↪  0.02419*N + 0.09263*S
210
211     corr_dict['20'] = 35.8368 + 0.7523*H - 0.2674*S - 0.4654*O -
        ↪  0.3814*Cl - 0.2802*N
212
213     return(corr_dict)
214
215
216 def corr_HHV_molar(HHV, C=0, H=0, O=0, S=0, N=0, A=0, Cl=0):
217     mass = C*12.01 + H*1.01 + O*16.00 + S*32.07 + N*14.01 + A +
        ↪  Cl*35.45
218     C = (C*12.01/mass)*100
219     H = (H*1.01/mass)*100
220     O = (O*16.00/mass)*100
221     S = (S*32.07/mass)*100
222     N = (N*14.01/mass)*100
223     A = A/mass * 100
224     Cl = (Cl*35.45/mass)*100
225
226     corr_dict = {}
227
228     corr_dict['1'] = 0.3383*C + 1.443*(H - (O/8)) + 0.0942*S
229
230     corr_dict['2'] = 0.3406*C + 1.443*H - 0.1532*O + 0.1047*S
231
232     corr_dict['3'] = 0.3391*(C - ((3/8)*O)) + 0.2386*(O*3/8) +
        ↪  1.444*(H - O/16)  + 0.1047*S
233
234     corr_dict['4'] = (0.373 - 0.00026*C)*C + 1.444*(H - O/10) +
        ↪  0.1047*S
235
236     corr_dict['5'] = 0.3391*C + 1.4337*H + 0.0931*S - 0.1273*O
237
238     corr_dict['6'] = (1.0632 + (1.486e-3)*O)*(C/3 + H - (O - S)/8)
239
240     corr_dict['7'] = (0.0152*H + 0.9875)*(C/3 + H - (O - S)/8)
241
242     corr_dict['8'] = 0.519*C + 1.625*H + 0.001*O**2 - 17.87
243
```

```
244     corr_dict['9'] = 0.3403*C + 1.2432*H + 0.0628*N + 0.1909*S -
        ↪  0.0984*O
245
246     corr_dict['10'] = 0.3391*(C - 0.75*(O/2)) + 1.444*(H -
        ↪  0.125*(O/2)) + 0.1047*S
247
248     if O <= 15:
249         HHV_c = 0.3361*C + 1.419*H - 0.1453*O + 0.0942*S
250     if O > 15:
251         HHV_c = 0.3361*C + 1.419*H - (0.1532 - 0.0007*O)*O + 0.0942*S
252     corr_dict['11'] = HHV_c
253
254     corr_dict['12'] = 0.3517*C + 1.1626*H + 1.047*S - 0.111*O
255
256     corr_dict['13'] = 0.3414*C + 1.4445*H - (N + O - 1)/8 + 0.093*S
257
258     corr_dict['14'] = 0.341*C + 1.323*H + 0.0685 - 0.0153*A -
        ↪  0.1194*(O + N)
259
260     corr_dict['15'] = 0.4373*C - 1.6701
261
262     corr_dict['16'] = -0.763 + 0.301*C + 0.525*H + 0.064*O
263
264     corr_dict['17'] = 0.328*C + 1.4306*H - 0.0237*N + 0.0929*S - (1 -
        ↪  A/100)*(40.11*H/C) + 0.3466
265
266     corr_dict['18'] = 0.352*C + 0.944*H + 0.105*(S - O)
267
268     corr_dict['19'] = 0.352*C + 1.507*H - 0.1384*O - 0.1485*C +
        ↪  0.02419*N + 0.09263*S
269
270     corr_dict['20'] = 35.8368 + 0.7523*H - 0.2674*S - 0.4654*O -
        ↪  0.3814*Cl - 0.2802*N
271
272     return(corr_dict)
273
274
275 def calc_HHV_mass(C=0, H=0, O=0, S=0, N=0, A=0, Cl=0):
276     my_dict = corr_HHV_mass(C, H, O, S, N, A, Cl)
277     HHV = (my_dict['6'] + my_dict['12'] + my_dict['20'])/3
278     return(HHV)
```

A.3 gasification_value_range

```
from database_read import *
import numpy as np
import matplotlib.pyplot as plt

#
# Adjustable values
#
h2_val_range = np.linspace(2.5, 4.8, 31)
heat_val_range = np.linspace(20, 100, 31)
el_dh_ratio = 2
steam_temp = 450
reactor_temp = 800
SFR = 1.75
feed_mat = 'BPA'
n_mem = 0.8


#
# Model loop and plotting
#
val_matrix = np.zeros([len(h2_val_range), len(heat_val_range)])
val_matrix_2 = np.zeros([len(h2_val_range), len(heat_val_range)])

for i in range(len(h2_val_range)):
    for j in range(len(heat_val_range)):
        val_gas = gasification_model(reactor_temp, SFR,
        ↪  H2_value=h2_val_range[i], dh_value=heat_val_range[j],
        ↪  feed=feed_mat, n_membrane=n_mem)
        val_comb_HOB =
        ↪  combustion_model(value_DH_eur=heat_val_range[j],
        ↪  max_steam_temp=steam_temp, mass_frac_turb=0,
        ↪  el_dh_val_ratio=el_dh_ratio, feed=feed_mat)
        val_comb_CHP =
        ↪  combustion_model(value_DH_eur=heat_val_range[j],
        ↪  max_steam_temp=steam_temp, mass_frac_turb=1,
        ↪  el_dh_val_ratio=el_dh_ratio, feed=feed_mat)
        val_matrix[i,j] = val_gas/max(val_comb_HOB, val_comb_CHP)
        val_matrix_2[i,j] =
        ↪  (heat_val_range[j]/h2_val_range[i])*val_matrix[i,j]


fig, ax = plt.subplots()
```

```
34 im = ax.imshow(val_matrix, origin='lower', aspect='auto')
35
36 # Label every other tick
37 xticks = np.arange(len(heat_val_range))[::2]   # every second tick
38 yticks = np.arange(len(h2_val_range))[::2]
39
40 ax.set_xticks(xticks)
41 ax.set_yticks(yticks)
42
43 ax.set_xticklabels([f"{heat_val_range[i]:.2f}" for i in xticks],
   ↪  rotation=45)
44 ax.set_yticklabels([f"{h2_val_range[i]:.2f}" for i in yticks])
45
46 # Axis labels
47 ax.set_xlabel("Heat Value: [EUR/MWh]")
48 ax.set_ylabel("H Value: [EUR/kg]")
49
50 # Colorbar
51 cbar = fig.colorbar(im, ax=ax)
52 cbar.set_label("Value ratio [SEK/kg(Feedstock)]")
53
54 plt.tight_layout()
55 plt.show()
56
57 masked_matrix = np.ma.masked_where(val_matrix < 1, val_matrix)
58
59 fig2, ax2 = plt.subplots()
60 im2 = ax2.imshow(masked_matrix, origin='lower', aspect='auto')
61
62 # Label every other tick
63 xticks = np.arange(len(heat_val_range))[::2]
64 yticks = np.arange(len(h2_val_range))[::2]
65
66 ax2.set_xticks(xticks)
67 ax2.set_yticks(yticks)
68
69 ax2.set_xticklabels([f"{heat_val_range[i]:.2f}" for i in xticks],
   ↪  rotation=45)
70 ax2.set_yticklabels([f"{h2_val_range[i]:.2f}" for i in yticks])
71
72 # Axis labels
73 ax2.set_xlabel("Heat Value: [EUR/MWh]")
74 ax2.set_ylabel("H Value: [EUR/kg]")
75
76 # Colorbar
77 cbar = fig2.colorbar(im2, ax=ax2)
78 cbar.set_label("Value ratio, masked value ratio < 1")
79
```

```
80 plt.tight_layout()
81 plt.show()
```

DEPARTMENT OF SOME SUBJECT OR TECHNOLOGY
CHALMERS UNIVERSITY OF TECHNOLOGY
Gothenburg, Sweden
www.chalmers.se

CHALMERS
UNIVERSITY OF TECHNOLOGY